Universidade de São Paulo

Instituto de Ciências Biomédicas

MARIA ISABEL MELO ESCOBAR

PrP^C e integrina α6 como moléculas centrais para orquestrar vias de adesão celular e ciliogênese na biologia do glioblastoma

Dissertação apresentada ao Programa de Pós-graduação em Biologia de Sistemas do Instituto de Ciências Biomédicas da Universidade de São Paulo, para obtenção do Título de Mestre em Ciências.

São Paulo

2022

MARIA ISABEL MELO ESCOBAR

PrP^C and integrin α6 as pivotal molecules to orchestrate cell adhesion and ciliogenesis pathways in glioblastoma biology

Dissertação apresentada ao Programa de Pós-graduação em Biologia de Sistemas do Instituto de Ciências Biomédicas da Universidade de São Paulo, para obtenção do Título de Mestre em Ciências.

Área de concentração: Biologia de Sistemas

Orientador: Profa. Dra. Marilene Hohmuth Lopes

Versão original

São Paulo

2022

CATALOGAÇÃO NA PUBLICAÇÃO (CIP)
Serviço de Biblioteca e informação Biomédica
do Instituto de Ciências Biomédicas da Universidade de São Paulo

Ficha Catalográfica elaborada pelo(a) autor(a)

Melo Escobar, Maria Isabel
PrPC and integrin ?6 as pivotal molecules to orchestrate cell adhesion and ciliogenesis pathways in glioblastoma biology / Maria Isabel Melo Escobar; orientadora Marilene H. Lopes. -- São Paulo, 2022.
63 p.

Dissertação (Mestrado)) -- Universidade de São Paulo, Instituto de Ciências Biomédicas.

1. glioblastoma. 2. integrina alfa 6. 3. proteina prion. 4. cilio primario. I. Lopes, Marilene H., orientador. II. Título.

UNIVERSIDADE DE SÃO PAULO

INSTITUTO DE CIÊNCIAS BIOMÉDICAS

Candidato(a): Maria Isabel Melo Escobar

Título da Dissertação/Tese: PrP^C and integrin α6 as pivotal molecules to orchestrate cell adhesion and ciliogenesis pathways in glioblastoma biology

Orientador: Marilene H. Lopes

A Comissão Julgadora dos trabalhos de Defesa da Dissertação de Mestrado/Tese de Doutorado, em sessão publica realizada a ...../...../....., considerou o(a) candidato(a):

( ) Aprovado(a) ( ) Reprovado(a)

Examinador(a): Assinatura: .....

Nome: .....

Instituição: .....

Examinador(a): Assinatura: .....

Nome: .....

Instituição: .....

Examinador(a): Assinatura: .....

Nome: .....

Instituição: .....

Presidente: Assinatura: .....

Nome: .....

Instituição: .....

Instituto de Ciências Biomédicas
ICB USP Excelência em Ensino e Pesquisa

Universidade de São Paulo
Comissão de Ética no Uso de Animais

CERTIFICADO

Certificamos que a proposta intitulada "Proteína prion e seus ligantes: potenciais alvos para terapia baseada em células-tronco de glioblastoma", protocolada sob o CEUA nº 6184230519, sob a responsabilidade de **Marilene Hohmuth Lopes** *e equipe; Rebeca Piatniczka Iglesia; Maria Isabel Melo Escobar; Gustavo Henrique Donãi Rodrigues Almeida; Mariana Brandã£O Prado* - que envolve a produção, manutenção e/ou utilização de animais pertencentes ao filo Chordata, subfilo Vertebrata (exceto o homem), para fins de pesquisa científica ou ensino - está de acordo com os preceitos da Lei 11.794 de 8 de outubro de 2008, com o Decreto 6.899 de 15 de julho de 2009, bem como com as normas editadas pelo Conselho Nacional de Controle da Experimentação Animal (CONCEA), e foi **aprovada** pela Comissão de Ética no Uso de Animais da Instituto de Ciências Biomédicas (Universidade de São Paulo) (CEUA-ICB/USP) na reunião de 30/09/2019.

We certify that the proposal "Prion protein and its partners: emerging targets for glioblastoma stem cell based-therapy", utilizing 216 Spontaneous mutant mice (216 females), protocol number CEUA 6184230519, under the responsibility of **Marilene Hohmuth Lopes** *and team; Rebeca Piatniczka Iglesia; Maria Isabel Melo Escobar; Gustavo Henrique Donãi Rodrigues Almeida; Mariana Brandã£O Prado* - which involves the production, maintenance and/or use of animals belonging to the phylum Chordata, subphylum Vertebrata (except human beings), for scientific research purposes or teaching - is in accordance with Law 11.794 of October 8, 2008, Decree 6899 of July 15, 2009, as well as with the rules issued by the National Council for Control of Animal Experimentation (CONCEA), and was **approved** by the Ethic Committee on Animal Use of the Biomedical Sciences Institute (University of São Paulo) (CEUA-ICB/USP) in the meeting of 09/30/2019.

Finalidade da Proposta: Pesquisa (Acadêmica)

Vigência da Proposta: 48 meses | Depto/Setor: Biologia Celular E do Desenvolvimento

Origem:	Biotério Central FMUSP			
Espécie:	Camundongo mutante espontâneo	sexo: Fêmeas	Idade ou peso:	3 a 6 meses
Linhagem:	Balb/c nude		**N amostral:**	216

São Paulo, 17 de fevereiro de 2020

Profa. Dra. Luciane Valéria Sita
Coordenadora da Comissão de Ética no Uso de Animais
Instituto de Ciências Biomédicas (Universidade de São Paulo)

Dr. Alexandre Ceroni
Vice-Coordenador da Comissão de Ética no Uso de Animais
Instituto de Ciências Biomédicas (Universidade de São Paulo)

ICB USP

Cidade Universitária "Armando de Salles Oliveira", Butantã, São Paulo, SP - Av. Professor Lineu Prestes, 2415 - ICB III - 05508 000
Comissão de Ética em Pesquisa - Telefone (11) 3091-7733 - e-mail: cep@icb.usp.br

CERTIFICADO DE ISENÇÃO

Certificamos que o Protocolo CEP-ICB nº **1023/2019** referente ao projeto intitulado: "***Impact of PrP^{c} and integrin α6 expression in stemness and invasiveness of glioblastoma stem-like cells***" sob a responsabilidade de ***Maria Isabel Melo Escobar*** e orientação do(a) Prof.(a) Dr.(a) ***Marilene Hohmuth Lopes,*** do Departamento de Biologia Celular e do Desenvolvimento, foi analisado pela **CEUA** - Comissão de Ética no Uso de Animais e pelo **CEPSH** – Comitê de Ética em Pesquisa com Seres Humanos, tendo sido deliberado que o referido projeto não utilizará animais que estejam sob a égide da Lei nº 11.794, de 8 de outubro de 2008, nem envolverá procedimentos regulados pela Resolução CONEP nº 466/2012.

São Paulo, 15 de abril de 2019.

Profa. Dra. **Luciane Valéria Sita**
Coordenadora CEUA ICB/USP

Profa. Dra. **Camila Squarzoni Dale**
Coordenadora CEPSH ICB/USP

À Deus, por me acompanhar em cada passo, sem Ele nada teria sido possível.

Aos meus pais, Fernando e Ximena, pelo apoio e presença constante em todos os momentos da minha vida; por me darem o suporte necessário para que alcançasse todos os meus objetivos.

À minha irmã, Laura, amiga e confidente, pela constante torcida.

AGRADECIMENTOS

Ao programa de Biologia de Sistemas do Instituto de Ciências Biomédicas da Universidade de São Paulo, em especial à minha orientadora Marilene Hohmuth Lopes pela direção e apoio incondicional, além do conhecimento compartilhado. Não poderia ter tido uma orientadora melhor, mais dedicada e compreensiva.

À Bárbara Paranhos Coelho, pós-doutoranda e mentora, pela guia e paciência nas diversas etapas do projeto e pela contribuição no desenvolvimento deste trabalho. Achei uma excelente mentora e amiga.

Aos colegas de laboratório, especialmente Jacqueline Boccacino e Giovanni Cangiano pela contribuição na bioinformática do projeto. Também à Camila Felix, Mariana Prado, Rebeca Iglesia, Rodrigo Alves, Clara Souza, Ailine Fortes, João Alves, Samuel Soares e nossa técnica Marlene, pela amizade e trocas de experiências e conhecimento.

Aos animais utilizados, que contribuem com o avanço da ciência.

Agradeço ao apoio da Fundação de Amparo à Pesquisa do Estado de São Paulo (FAPESP) processos 2019/11097-1/2018/15557-4 pelo auxílio financeiro que proporcionou ao Laboratório de Neurobiologia e Células-tronco, a infraestrutura adequada, insumos necessários e equipamentos modernos para a realização deste trabalho.

RESUMO

Melo Escobar, M.I. PrP^C and integrin α6 as pivotal molecules to orchestrate cell adhesion and ciliogenesis pathways in glioblastoma biology. [dissertação (Mestrado em Biologia de Sistemas)]. São Paulo: Instituto de Ciências Biomédicas; Universidade de São Paulo, São Paulo; 2021.

O glioblastoma (GBM), tumor cerebral maligno primário mais comum em adultos regido por células-tronco de glioblastoma (GSCs), é caracterizado pela heterogeneidade celular, resposta limitada à terapia e recorrência tumoral. As interações célula-matriz extracelular influenciam diferentes vias de sinalização que determinam fortemente a proliferação, diferenciação e migração de células GBM. As integrinas, importantes mediadores da interação entre as células do GBM e o microambiente circundante, compartilham domínios específicos da superfície celular do tipo *lipid rafts* com a proteína prion celular (PrP^C). PrP^C é uma glicoproteína de superfície celular capaz de organizar complexos multiproteicos relacionados à manutenção de GSCs, dos quais integrina α6 (ITGA6) pode ser um componente e participar de eventos integrados de adesão celular e sinalização celular em células GBM. Para investigar a potencial associação entre PrP^C e ITGA6 em amostras de GBM, combinamos experimentos *in vitro* com análises de transcriptoma e proteômica para verificar as consequências da modulação da expressão de PrP^C e/ou ITGA6 na biologia de GBM. Nossos resultados sugerem que ITGA6 e PrP^C modulam sua expressão mutuamente e são co-localizadas em células de GBM. O silenciamento da ITGA6 desencadeou a regulação positiva da expressão de PrP^C e vice-versa em linhagens de GBM. Notavelmente, análises de perfis de transcriptoma e proteoma identificaram genes diferencialmente expressos (DEGs) e proteínas relacionadas à ciliogênese (formação de estrutura solitária e imóvel de membrana responsável pelo controle de diferentes fenômenos celulares) e à processos de adesão celular em células de GBM que expressam altos níveis de ITGA6 ou nocautes (KO) para PrP^C. Entre os DEGs obtidos *ITGA6, PRNP, PROM1*, *GLI1*, *PDGFRA, TUBA1A* e *DNAHs* se apresentam como candidatos de uma rede gênica associada à processos de ciliogênese e adesão celular em GBM. Nossos resultados revelam um papel emergente para ITGA6 e PrP^C no estado ciliado das células GBM e podem apontar novas estratégias para inibir a gliomagênese.

Palavras chave: glioblastoma, integrinas, integrina alfa 6, proteína prion, células-tronco de glioblastoma, adesão celular, cílio primário.

ABSTRACT

Melo Escobar, M.I. PrP^C and integrin α6 as pivotal molecules to orchestrate cell adhesion and ciliogenesis pathways in glioblastoma biology. [Dissertation (Master of Science in Systems biology)]. São Paulo: Instituto de Ciências Biomédicas; Universidade de São Paulo, São Paulo; 2021.

Glioblastoma (GBM), the most common primary malignant brain tumor, is dominated by Glioblastoma Stem Cells (GSCs) and characterized by cellular heterogeneity, limited response to therapy, and tumor recurrence. Cell-to-extracellular matrix interactions influence different signaling pathways that strongly determine the proliferation, differentiation, and migration of GBM cells. Integrins, important mediators of interaction between GBM cells and the surrounding microenvironment, share specific cell surface domains, such as lipid rafts, with the cellular prion protein (PrP^C). PrP^C is a cell surface glycoprotein, able to organize multiprotein complexes related to GSCs maintenance, of which integrin α6 (ITGA6) might participate towards integrated cell adhesion and cell signaling events in GBM cells. To investigate the potential association between PrP^C and ITGA6 in GBMsamples, we combined *in vitro* experiments with both transcriptome and proteomic analyses to assess the modulation of expression of either PrP^C or ITGA6 in GBM biology. Our results suggest that ITGA6 and PrP^C modulate their expression mutually and are co-localized in GBM cells. Furthermore, ITGA6-knockdown GBM cells triggered upregulation of PrP^C expression and vice-versa in U251 cells. Notably, transcriptome and proteome profiles analyses identified differentially expressed genes (DEGs) and proteins related to ciliogenesis (formation of a single and immobile membrane structure responsible for the control of different cellular phenomena) and cell adhesion processes in cells expressing high levels of ITGA6 and in PrP^C knockout (PrP^C-KO) GBM cells. Among the retrieved DEGs *ITGA6, PRNP, PROM1*, *GLI1*, *PDGFRA*, *TUBA1A*, and *DNAHs* pose as candidate interactors at the intersection of ciliogenesis and cell adhesion processes in GBM. Our findings reveal an emerging role for ITGA6 and PrP^C in the ciliated state of GBM cells and may point out novel strategies to inhibit gliomagenesis.

Keywords: glioblastoma, integrins, integrin alpha 6, prion, glioblastoma stem cells, cell adhesion, primary cilia.

LIST OF FIGURES

LIST OF TABLES

LIST OF ABBREVIATIONS

bFGF	Fibroblast Growth Factor
BP	Biological processes
CC	Cell components
CPM	Counts per million
DEGs	Differentially expressed genes
DEPs	Differentially expressed proteins
ECM	Extracellular matrix
EGF	Epidermal Growth Factor
FBS	Fetal bovine serum
GBM	Glioblastoma
GSCs	Glioblastoma stem cells/Células-tronco de glioblastoma
GO	Gene ontology
HOP	Heat shock organizing protein
ITGA6	Integrin alpha 6
ITGA6 KD	Integrin alpha 6 Knockdown
ITGA6 OE	Integrin alpha 6 Overexpression
KO	Knockout
NSCs	Neural stem cells
ORA	Overrepresentation analysis
PDX	Patient-derived xenograft
PrP^{C}	Cellular prion protein
PrP^{C}-KO	Knockout cells for the cellular prion protein
PrP^{SC}	Prion Protein Scrapie
RNA-Seq	RNA sequencing
RT-qPCR	Quantitative reverse transcription PCR
Shh	Sonic Hedgehog
STRING	Search Tool for the Retrieval of Interacting Genes/Proteins
TCGA	The Cancer Genome Atlas
TGF- β	Transforming growth factor β
WT	Wild-type

TABLE OF CONTENTS

1 INTRODUCTION

Glioblastoma (GBM) is one of the most common and lethal central nervous system tumors, classified as grade IV in histological malignancy and composed of genetically and phenotypically heterogeneous cells (1)(2). GBM cells migrate from the primary tumor bulk to the adjacent normal tissue by infiltrating and degrading physical barriers, such as basement membranes, extracellular matrix (ECM), and cell junctions (3). The typical treatment for GBM begins with surgical resection of the tumor. Then, patients undergo radiotherapy, followed by adjuvant temozolomide therapy. To date, this treatment procedure is the most effective as it increases the median overall survival from 12 months to 14.6 months (4).

The highly heterogeneous profile of GBM requires assessment at different levels of information flow from genome to proteome. These high-throughput assays retrieve gene annotation from genetic databases and allow cross-validation by integrating complementary experimental data. An increasing number of sequencing data are being deposited in public databases such as The Cancer Genome Atlas (TCGA), as well as proteomics data like Proteomics Identifications Database (PRIDE), a public data repository of mass spectrometry. These datasets have allowed the classifications of gliomas, especially GBM, to facilitate diagnosis and treatment (5)

The cellular prion protein (PrP^{C}) is a cell-surface glycoprotein known primarily for its critical role in the pathogenesis of neurodegenerative disorders such as the transmissible spongiform encephalopathies caused by its conformational conversion into an aggregated, β-sheet-rich isoform called PrP^{Sc} (scrapie prion protein) (6). Loss of normal PrP^{C} function might be an essential factor of neurodegenerative processes, and, thus, significant research efforts have been directed toward establishing the physiological functions of PrP^{C} (7). PrP^{C} interaction with different ligands on the plasma membrane (receptors NCAM, caveolin), soluble factors such as the heat shock organizing protein (HOP), and extracellular matrix molecules such as vitronectin and laminin, have led to consider this glycoprotein as a component of a dynamic platform modulating the assembling of signaling modules on the cell surface (8). PrP^{C} has been pivotal in regulating proliferation, apoptosis, invasion, metastasis, and drug resistance in several cancer types, such as gastric tumors, colorectal cancer, breast cancer, and GBM (9)(10). Our group recently described the association of PrP^{C} in the regulation of proliferation, self-renewal, and differentiation of glioblastoma stem-like cells (GSCs), a vastly proliferative subset of cells that contribute to tumor initiation and therapeutic resistance (11). Neurospheres derived from

GBM cultures have been reported to recapitulate the properties of GSCs and express stem cells markers such as GFAP, CD133, Nestin, Nanog, CD44, and CD90 (12). PrP^C expression has been directly correlated with the proliferation rate of these cells. Likewise, the ability to form neurospheres and *in vivo* tumorigenicity were significantly inhibited in PrP^C down-regulated cells (10). Moreover, our group studied the interaction of PrP^C and HOP, a co-chaperone that associates with heat shock proteins Hsp70 and Hsp90, facilitating the folding and maturation of newly-synthesized proteins including in GBM cells (13)(14). Additionally, our group showed that PrP^C and HOP expression are directly related to GBM aggressiveness (15).

Novel interacting protein partners of PrP^C might provide an insight into its enigmatic physiological functions. PrP^C has been described to participate in signal transduction events by interacting with plasma membrane proteins. Its binding to ECM proteins, including laminin and vitronectin, has been shown to mediate neuritogenesis (16). PrP^C exhibits high affinity as a saturable receptor for laminin and binds at the carboxyterminal decapeptide of the laminin Ɣ-1 chain (17). Laminin not only creates a complex with PrP^C that is essential for neuronal plasticity mechanism, but also regulates neuronal differentiation through its interaction with integrins. The laminin-integrin complex has been reported to promote the migration of neurons both *in vitro* and *in vivo*, and to mediate neuronal and axonal regeneration (18). Strikingly, PrP^C expression has also been identified combined with MGr1-Ag/37LRP, a laminin receptor precursor, which is predictive of poor prognosis in gastric cancer (19).

Figure 1 - PrP^C, integrin a6 and potential partners

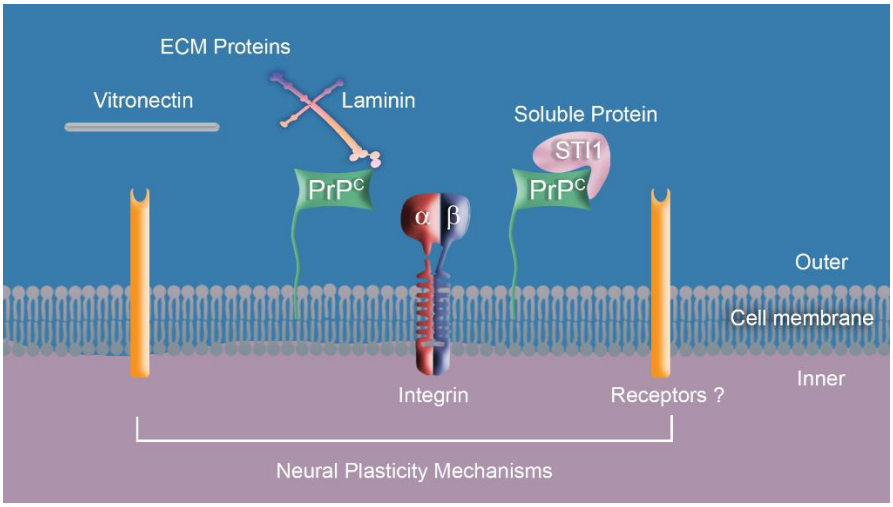

PrP^C is associated with lipid raft microdomains of the plasma membrane, where it combines with several protein partners, including cell adhesion and signaling molecules. Own work.

On the other hand, an important integrin for stem cell biology is integrin α6 (ITGA6), which for instance, regulates neural stem cells (NSCs) growth and plays a pivotal role in maintaining their adhesion to the ventricular zone, thereby ensuring proper NSC division (20). This protein is not only essential for cell adhesion, but it also may be the only biomarker able to participate in stemness maintenance and is commonly found in more than 30 different populations of stem cells, including NSCs, myogenic stem cells, and GSCs (20)(21)(22). Specifically, integrin α6-positive GSCs express the integrin β1 co-receptor, with a extracellular expression of the ligand laminin, suggesting the presence of a fully active integrin signaling unit (22). Furthermore, it was demonstrated that reducing ITGA6 expression using siRNA or blocking laminin-ITGA6 interaction with a specific antibody decreases proliferation of GSCs and their neurosphere formation ability and increases cell death (22). More recently, ITGA6 has been related to the ZEB1 transcriptional network to sustain DNA damage response in GBM (23).

Main features for ITGA6 were established regarding its expression in GSCs (22): First, high levels of ITGA6 expression were found in the perivascular niche of GSCs, and it was co-expressed with CD133, a well-known marker for cancer stem cells (22). Moreover, it was determined that CD133+/ ITGA6+ and CD133-/ ITGA6+ GSCs formed spheres with greater efficiency than cells negative for ITGA6 (22). At last, targeting ITGA6 inhibits GSCs cell growth and abrogates neurosphere formation. The displayed characteristics may support the hypothesis that ITGA6 promotes the maintenance of GSCs.

Integrins as major laminin receptors have been reported to act through the same signal transduction pathway as PrP^C, which arouses the question of whether there might be a certain interaction. For instance, PrP^C-knockout neurons displayed greater dependence upon integrins for axonal outgrowth than their respective wild-type cells (24). Additionally, PrP^C as a GPI-anchored protein has been linked to clathrin-mediated endocytosis and caveolae-based transport of integrins (25). Noteworthy, a study reported a decrease in E-cadherin and ITGA6 expression in PrP^C-silenced GSCs neurospheres (11). In addition, a high co-localization of integrin β1 and PrP^C signalizes a potential relationship with the dimer α6β1. Depletion of PrP^C also affected the localization of β-catenin, which is crucial for the regulation and coordination of cell adhesion. Moreover, β-catenin activation is essential for the Wnt pathway in GBM (26) since it is upregulated and leads to the maintenance of stemness in GSCs (27)(28). Altogether, the prior evidence suggests the tight relationship between cell adhesion and cell signaling in the biology of GBM cells, whereof ITGA6 and PrP^C are relevant participants.

PrP^C has been found as a hub for an extensive range of multicomponent signaling modules in which ITGA6 might be involved. The preferential location of PrP^C on the cell membrane favors its function as a scaffold protein for extracellular matrix proteins, cell surface receptors, and cytoskeletal multiprotein complexes (30). PrP^C has been reported to be involved in forming multiprotein complexes for intracellular signaling and actin cytoskeleton remodeling. PrP^C is able to alter the turnover of focal adhesions and its silencing to increase the stability of the actin network, proving that PrP^C's contribution to neuronal polarization relies on its modulatory action on integrin-ECM interactions (16). The role of integrins and PrP^C at the core of cell adhesion and signaling structures has been described before. The activation of integrin receptors was associated with Ca^{2+} influx that affects membrane trafficking and reorganization of the growth cone in neuron cells; whereas PrP^C-KO leads to a reduction in the number and trafficking of vesicles containing N-cadherin, resulting in impaired downstream signaling, ultimately leading to smaller growth cone and elongation failure (31). Another example was identified in the uropod, a structure that forms on one edge of the migrating leukocyte for cell polarization and contains cholesterol-rich membrane domains, β1 integrins, and other adhesion receptors (32). PrP^C silencing alters RhoA activation and inhibits monocyte uropod formation, increasing chemotaxis and motility on β1 integrin ligands (33).

Other common features between ITGA6 and PrP^C have been reported. For instance, PrP^C may interact with the cell surface protein CD44, a marker for several cancer stem-like cells (11) (unpublished results), while integrin α6 is co-expressed with conventional GSC markers and enriches for GSCs (22). Moreover, PrP^C has been shown to control integrin β1 adhesiveness by modulating ligand-induced changes in integrin activation (33)(11). PrP^C depletion does not affect total β1 integrin expression levels, however, this integrin is co-localized with PrP^C on the cell surface. Hence, these data suggest that PrP^C may be able to recruit cell adhesion molecules to the cell surface of GSCs, supporting the rationale of PrP^C modulating invasion-related processes (11). On the other hand, integrin α6 mediates a physical link between the tumor cells and the ECM for cell migration, thus modulating the infiltrative capacity of malignant cells (34). Altogether, PrP^C and integrin α6 exhibit shared effects on GSCs behavior, such as high expression as identifying markers of stem-like cells, co-expression with other markers for stem-like cells, interaction with laminin, and great influence in anchorage-dependent cell processes (35).

The heterogeneous, invasive and aggressive nature of GBM makes biological processes such as cell adhesion and cell signaling of great interest. Since primary cilia regulate cell cycle

and signaling transduction, abnormal cilia have been reported to be involved in cancer progression and tumorigenesis. The primary cilium is a conserved mechanosensory hub for cell signaling, in which adhesion molecules participate as well (37). Loss or decrease of cilia is a commonly described feature in malignant tumors such as pancreatic adenocarcinoma, breast cancer, melanoma, or renal cell carcinoma, so primary cilium has been proposed to act as a tumor suppressor organelle (38). Furthermore, cancers exhibit alterations in several signaling cascades, especially regarding the upregulation of Shh (sonic hedgehog) signaling, which has been widely characterized as a cilia-regulated pathway (39). Regarding malignant astrocytic tumors like GBM, the primary cilium from astrocytes was reported to act as the central hub that integrates and transduces the Shh signaling to regulate cell survival under stress conditions (40).

Currently, little evidence on cilia-dependent GBM is available, but different recent works have considered whether primary cilia can affect GBM proliferation. A large study of GBM biopsies and primary human GBM cell lines reported that small subpopulations in all cells and tissues have mature primary cilia, but there were found non-ciliated cells with abnormal centrioles as well (41). The function of primary cilia in GBM has been described as dualistic (42) due to the ciliary loss being linked to increased (43) but also decreased proliferation (44). The responsiveness of primary cilia to different extracellular conditions could constitute an essential adaptive mechanism to modulate tumor progression (45). It plays a critical role within the cell cycle and signaling transduction (46)(47), regulating the main signaling pathways involved in GBM biology; such as Shh, transforming growth factor-beta (TGF-β), Notch, PDGFRα (48)(49)(50) and integrin signaling (51). Since many diseases associated with this organelle (ciliopathies) display neurological features (52), it may also participate in GBM tumorigenesis and progression (45). As an example, it has been shown that patient-derived GBM cell lines can transduce Shh-mediated signaling through primary cilia to promote cell proliferation (53). More importantly, the signaling function of the primary cilia has been associated with the expression, secretion, and proteolytic remodeling of the extracellular matrix (54), as well as altered integrin expression (55). Primary cilia have been described as integrators of extracellular ligand-based signalling and cellular polarity, which modulate neuronal cell fate and migration differentiation (56). It has been shown that under normal conditions, integrins co-localize with the primary cilium (57), and mechanical stimuli have been shown to modulate integrin-mediated signals (58).

The role of PrP^C in cell signaling processes has also become of interest (30), since PrP^C is responsible for recruiting spatially restricted sets of binding molecules involved in specific

signaling; mediation of the crosstalk of signaling pathways; reciprocal allosteric regulation with binding partners, and compartmentalized responses (8) (15). Regarding the role of PrP^C in the signaling structure that is the primary cilium, its enrichment has been reported at the base of the primary cilium in stem and progenitor cells from the central nervous system (59) and could constitute an important regulator of this sensory organelle that is enriched for a number of receptors and ion channels.

Based on those findings, we hypothesize that ITGA6 and PrP^C can orchestrate key signaling pathways required for GBM biology. Evaluation of the association between ITGA6 and PrP^C contributes to a better understanding of the behavior of GBM cells and to elucidating relevant mechanisms for the development of new GBM-targeted therapy.

2 OBJECTIVES

To evaluate the potential association between PrP^C and ITGA6 in GBM biology via experimental data and complementary transcriptome and proteome analysis.

2.1 SPECIFIC OBJECTIVES

I Evaluate ITGA6 and PrP^C expression across GBM cell lines in neurosphere and monolayer condition and in patient cells.

II Validate ITGA6 and PrP^C expression in knockdown, knockout and overexpressed conditions in GBM cell lines.

III Evaluate the role of ITGA6 and PrP^C in cell adhesion and cell signaling events of GBM biology via transcriptome and proteome analysis.

3 MATERIAL AND METHODS

3.1 Meta-analysis

RNA sequencing (RNA-seq) data of GBM cells were obtained from The Cancer Genome Atlas (TCGA) database using TCGA biolinks in R. Count data of 156 primary GBMs was normalized to counts per million (CPM) utilizing edgeR, and the results were converted to the log10(CPM+1) scale, classifying the samples by ITGA6 expression quartiles. The first quartile was defined as ITGA6-Low (n=39) and the fourth one as ITGA6-High (n=39). Mann-Whitney statistical test ($p<0.05$) was used to confirm if these groups showed different expressions of ITGA6. Then, raw counts of these groups were used for differential expression analysis in DESeq2, comparing ITGA6-High samples with ITGA6-Low ones (control). The differentially expressed genes (DEGs) were visualized through Enhanced Volcano and filtered according to log2foldchange <=-1 and >=1 and padj<0.05, resulting in a list of 1454 DEGs, which were subsequently used for overrepresentation analysis (ORA) in clusterProfiler. ORA was carried out using Gene Ontology, KEGG, Reactome, WikiPathways, and Disease Ontology databases and defining padj<0.05 as statistically significant. The most relevant processes and pathways were illustrated through bar plots in GraphPad Prism 8 in terms of -log10(padj). Gene and protein interactions were assessed using the Search Tool for the Retrieval of Interacting Genes (STRING; https://string-db.org/, accessed February 17, 2021) and inBio Discover™ (https://inbio-discover.com/, accessed February 23, 2021) using DEGs as input. For correlation verification, Spearman correlations between genes of interest were computed with log10(CPM+1)-normalized counts and plotted using corrplot in R, according to $p<0.05$. Kaplan-Meier survival curves for *ITGA6* and *PRNP* were obtained from the Gliovis portal (http://gliovis.bioinfo.cnio.es), selecting TCGA datasets of adult GBM samples.

3.2 Cell culture

The human U87 and U251 glioblastoma cell lines (ATCC) were grown as both neurosphere and monolayer cultures. Neurospheres were cultured in DMEM-F12, supplemented with B27 (Cat No. 17504-044; Gibco, Gaithersburg, MD, USA; 1:50) in the presence of 20 ng/ml epidermal growth factor (EGF; Cat No. E4127; Sigma Aldrich, St. Louis, MO, USA) and basic fibroblast growth factor (bFGF; Cat No. F0291; Sigma

Aldrich) at 37 °C under 5% CO2 to form neurospheres. The medium was replaced every 2 days. Monolayer cells were cultured in DMEM-Low Glucose medium supplemented with 10% Fetal Bovine Serum (FBS) and 1% antibiotic-antimycotic (Cat No. 15240062; Gibco). For dissociation, cells were treated with 0.25% trypsin (Cat No. 25200-056; Gibco) in HBSS (Cat No. 14170-112; Gibco) for 5 min at 37 °C. Trypsin was washed out, and the cells were mechanically dissociated and plated for distinct assays. Patient-derived xenograft cells were kindly provided by Dr. Tiago Goss from AC Camargo Cancer Center (ACCCC) and cultured as monolayer and neurosphere as described above. This project was approved by both Institutions (Ethical Committee Approval Certified Numbers: ACCC#1692/12 and Institute of Biomedical Sciences#3.924.747).

U87 and U251 PrP^{C}-Knockout cells (Clone 5 and 2-2, respectively) were generated by our group via CRISPR-Cas9 using the NM_00311.3 human genome sequence of the *PRNP* gene to design the guide RNA (sgRNA) and cloned it in a px330-U6-GFP vector (Addgene) following the manufacturer's instructions for transfection. PrP^{C}-KO cells were cultured in monolayer and neurospheres as described above. Herein, all letters of gene and protein symbols are in the upper case, and genes symbols are italicized to differ from proteins.

ITGA6-knockdown was performed using 30 nM ITGA6 esiRNA (Cat No. EHU088861-20UG; Mission). Cells were transfected using Nucleofector device from Lonza and the Amaxa mouse Neural Stem Cell KIT (Cat No. VPH-1001; Lonza) according to the manufacturer's instructions.

ITGA6-overexpression was performed with plasmid Human ITGA6 transcript variant 2 ORF mammalian expression plasmid, C-GFPSpark 100 ng/μL. Cells were transfected using Nucleofector device from Lonza and the Amaxa mouse Neural Stem Cell KIT (Cat No. VPH-1001; Lonza) according to the manufacturer's instructions.

3.3 RNA sequencing data analysis

U87 and U251 GBM cell lines were used for RNA-seq analysis, and sequencing was performed in a previous study of our group (data not shown). Briefly, RNA was extracted with the RiboPure RNA Purification kit (Ambion), according to the manufacturer's instructions. The following groups were used: monolayer U87 wild-type (WT); monolayer U87 PrP^{C} KO (Clones 5 and 211); monolayer U251 WT; monolayer

U251 PrP^C KO (Clones 11 and 22). After RNA extraction, approximately 4.5 µg of RNA was used to generate the RNA-seq libraries. Both library preparation and the RNA sequencing were outsourced by Indegene, using the NextSeq 500/550 High Output v2.5 kit (Illumina).

Our bioinformaticians collaborators, Professor Helder Nakaya (FCF-USP) and Dr. Frederico Ferreira (INCOR), performed the quality control of the sequencing output and the alignment of the reads to the Homo sapiens genome (GRCh38). FastQC was used for a general quality control check, Cutadapt was used for trimming, while TopHat and Bowtie were used for the alignment. The remainder of the data analysis was performed by an outsourced service (Duna Bioinformatics) and members of our laboratory, as follows. First, to verify similarity among the samples, principal component analysis was used. After that, differential expression analysis was performed with DESeq2, and genes with p or padj< 0.05 and/or |log2(Fold change)|≥2 were considered differentially expressed. Then clusterProfiler's compareCluster was used to ascertain which pathways and processes displayed alterations between the pairwise comparisons. Finally, using the DEGs as input, ORA was performed for Gene Ontology, KEGG, Reactome, WikiPathways, and Disease Ontology databases, defining padj<0.05 as the statistical cutoff.

3.4 Real-time quantitative PCR (RT-qPCR)

RT-qPCR technique was used for transcript expression assessment. Briefly, cDNA was synthesized from 2µg of total RNA treated with DNAse I in a 20µl reaction using SuperScript IV VILO Master Mix (Thermo Fisher Scientific). The RT-qPCR was performed with Platinum SYBR Green SuperMix (Invitrogen) and analyzed using StepOne Plus (Thermofisher). qRT–PCR analysis for U87 and U251 cells were performed in biological and technical triplicates. Relative gene expression was calculated by the $2^{-\Delta\Delta Ct}$ method, and the reference gene for normalizing the data was human TATA-Box Binding Protein (TBP). Unpaired t-test and One-Way ANOVA statistical analysis was performed using GraphPad Prism software.

Table 1 - List of the primer sequences used for RT-qPCR

Gene name	Gene sequence (5'-3')
ITGA6-F	ATGCACGCGGATCGAGTTT
ITGA6-R	TTCCTGCTTCGTATTAACATGCT
LAMA5-F	GGCTTTCCCCGAGCTGTACT
LAMA5-R	AGGGTCCCACCGTAGGATGA
THBS2-F	AGCTCCTCTTCAATCCCCGC
THBS2-R	AGGCGTCACCCTCTCCATTG
EPHA4-F	ACTTGGAAGGCGTGGTCACT
EPHA4-R	CCCAGACCCAATGCCACGAA
EPHB4-F	CTCCTTCCTGCGGCTAAACG
EPHB4-R	GGACGTAGCTCATCTCGGCA
TIMP3-F	CTTCGGCACGCTGGTCTACA
TIMP3-R	GCCATCATAGACGCGACCTGT
NCAM1-F	CAGCCAGTCCAAGGGGAACC
NCAM1-R	ACGGGAGCCTGATCTCTGGT
PRNP in del.-F	CCTGGAGGCAACCGCTAC
PRNPin del.-R	TCGGCTTGTTCCACTGACTG
DNAH1-F	TGTGGACACCTTGCCTCCAG
DNAH1-R	CCAGCCGAAGCTCCCTTCAA
PDGFRA-F	TGTGTCCACCGTGATCTGGC
PDGFRA-R	TTCACGGGCAGAAAGGTACTG
GLI1-F	TGACGCCCATGTGACCAAAC
GLI1-R	TGGCTGTGGCTTCATGGCA
TUBA1A-F	GAAGCAGCAACCATGCGTGA
TUBA1A-R	GCCGTGTTCCAGGCAGTAGA
TBP-F	AGGATAAGAGAGCCACGAACCA
TBP-R	CTTGCTGCCAGTCTGGACTGT

3.5 Immunoblotting

Protein extracts from WT, PrP^{C}-KO monolayer and spheres of U87 and U251 cells and transfected cells, were obtained by incubation in RIPA buffer (50mM Tris HCl; 150mM NaCl; 2mM EDTA; 0,5% Triton X-100; 0,5% deoxycholate), along with 10% protease inhibitors and 5% phosphatase inhibitors for 30 min on ice. Proteins were quantified by the Bradford method (Pierce Inc Rockford, IL, USA). Equal amounts of total cellular lysates (25-30 μg) were separated by SDS-PAGE in Mini-PROTEAN® TGX™ Precast Gels 4-20% polyacrylamide (BioRad) and transferred on a PVDF membrane using Trans-Blot Turbo (Biorad). The membranes were blocked with 5% freeze-dried skimmed milk in a saline solution buffered with Tris and 0.1% Tween-20

(TBST) for 1h. The antibodies used were anti-ITGA6 (Cat No. 100497-T10; Sino-biological; 1:500), anti-PrP^C (Cat No. MAB1562; Millipore; 1:500), anti-EGFR (Cat No. 4267S; Cell signaling; 1:1000). Antibody against actin (Cat No. A2103; Sigma Aldrich; 1:5000) was used for protein loading control. Antibodies were incubated in a 5% solution of bovine serum albumin overnight at 4 ° C. The following day, membranes were washed 3x with TBST and incubated with anti-mouse (1:3000) or anti-rabbit (1:3000) in blocking solution for 1 hour at room temperature.

3.6 Flow Cytometry

Cells underwent dissociation and 30 minute-blocking (5% BSA in PBS) on ice, followed by incubation with anti-ITGA6 (Cat No. 100497-T10; Sino Biological; 1:50) diluted in 0,5% BSA in PBS for 1 hour on ice. In addition, secondary antibody Alexa Fluor 546 goat anti-rabbit (1:100, Cell Signaling) was added for 1 hour on ice. Samples were analyzed on a FACSCanto II flow cytometer (BD Biosciences).

3.7 Immunofluorescence staining

Monolayer cells and whole neurospheres were harvested, plated on coverslips previously treated with gelatin 0.2%, and fixed in 4% paraformaldehyde. Coverslips were blocked for 1 h at RT with 5% BSA plus 0.3% triton in PBS. Coverslips were incubated overnight at RT with anti- PrP^C (Cat No. MAB1562; Millipore; 1:100), anti-ITGA6 (Cat No. 100497-T10; Sino-biological; 1:100), anti-CD44 (Cat No. 3570S; Cell signaling; 1:100) and anti- α -tubulin (Cat No. 11224; Proteintech; 1:100) in 1% BSA 0.1% triton in PBS. After washing, coverslips were incubated for 1 h at RT with anti-mouse Alexa-488 (Cat No. A21202; Invitrogen; 1:1500) or anti-rabbit Alexa-546 (Cat No. A10040; Invitrogen; 1:500), and stained with DAPI (Cat No. D1306; Invitrogen; 1:500) for nuclei. Cells were imaged on a Leica TCS SP2 II laser scanning confocal system.

3.8 Immunostaining and quantification of ciliated cells

U251 GBM cells were immunostained with anti- alpha-tubulin (Cat No. 11224; Proteintech; 1:100). A triplicate of 5x5 image tiles was captured on a Leica TCS SP2 II laser scanning confocal system and stitched to generate a high-resolution image covering a larger area of multiple continuous fields. We quantified the numbers of

ciliated cells by counting the number of DAPI-labeled nuclei and cilia in each field. The percentage of ciliated cells was calculated as the number of cilia/number of DAPI-labeled nuclei for each field.

3.9 Proteomic analysis

GBM proteomics data were obtained from the Proteomics Identifications Database (PRIDE), and 2 datasets were chosen: one comparing adherent versus spheroid GBM proteomics (PRIDE Project PXD008244) (59); another were samples from human GBM tissue (PRIDE Project PXD015545) (60). For the PXD008244 dataset, samples were first filtered for contaminants for the reverse database and the ones only identified by site. Then, intensity values were transformed by log2(intensity), and the groups were determined. The authors used several GBM cell lines to generate these samples and pooled them for the mass spectrometry readings. Groups were determined based on the replicates the authors had separated, with 4 adherent and 4 spheroid samples. Following log transformation of the intensity, the Benjamini-Hochberg method was used to determine the differentially expressed proteins (DEPs), comparing the spheroid group with the adherent group (control), with a False Discovery Rate (FDR) = 0.05 and a s0 = 0.1. As described above the 570 DEPs obtained were subsequently used for overrepresentation analysis (ORA) in clusterProfiler. The most relevant processes and pathways were illustrated through bar plots in terms of -log10(padj). DEPs were also filtered by genesets of cilium-related processes from the Gene Ontology and Reactome databases, obtained from the GSEA website (http://www.gsea-msigdb.org). The genesets used are described in Supplementary Table 1. Protein-protein interactions were assessed using the Search Tool for the Retrieval of Interacting Genes (STRING).

The PXD015545 dataset contained 6 sets with 6 samples each, tagged with 6 different tandem mass tags (TMT). The GBM Global sets 1 to 6 were selected for analysis. First, samples were filtered for contaminants, for reverse database, and the ones only identified by site. Next, samples were normalized by dividing each sample from each set by the Global Internal Standard (GIS) of the respective set. Following this, each ratio obtained by the normalization was log-transformed [log2(ratio)]. Next, samples of normal tissue, which were 4, were removed, remaining GBM 26 samples. Following this, samples were filtered by either their ITGA6 or PrP^{C} log2(ratio) and

separated into ITGA6 or PrP^C high expression and low expression groups. For the comparison between ITGA6 high expression (n=6) versus ITGA6 low expression (n=6, control group), the Permutation-based FDR method was used to determine the DEPs, with FDR = 0.05 and s0 = 0.1. For the comparison between PrP^C high expression (n=6) versus PrP^C low expression (n=6, control group), the Benjamini-Hochberg method was used to determine the DEPs, with FDR = 0.05 and s0 = 0.1. DEPs obtained were subsequently used for ORA analysis, followed by filtering by cilium-related processes, and submitted for STRING analysis, as described above.

3.10 Statistical Analysis

Data graphs are presented as means ± SEM (standard error of the mean) or geometric means (for RT-qPCR). Statistical analyses were conducted using the GraphPad Prism software. Distinct tests were used to assess statistical significance according to data distribution (Student's t-test and Mann–Whitney test). Statistical significance was set at $p < 0.05$.

4 RESULTS

As our group had previously described the potential role of PrP^C in regulating the cell surface stability of cell adhesion molecules in GBM (11)(30), we executed transcriptome and proteome profiling, as well as *in vitro* assessment in order to reveal new insights in GBM biology.

4.1 Transcriptome analysis of PrP^C-KO U87 and U251 GBM cells

The transcriptome analysis was based on the gene expression profile of PrP^C knockout (PrP^C-KO) clones from U87 and U251 GBM cells by conducting bulk RNA-seq analysis. Briefly, wild-type (WT) and PrP^C-KO clones were cultured and sequenced using the Illumina system. Subsequently, output data was processed, and differentially expressed genes (DEGs) were defined for both cell lines (Fig. 2A). To explore the biological roles of these DEGs, we performed an overrepresentation analysis according to different signaling pathway databases, namely KEGG, DOSE, Reactome, and Gene Ontology (GO) (Fig. 2A).

Up to 1295 DEGs were found in U87 PrP^C-KO cells relative to their WT counterparts (Fig. 2C). GO terms associated with ECM organization, and collagen biosynthesis were overrepresented in this cell subset (Fig. 2C). To a lesser extent, there were also terms related to integrins, fibronectin, glycosaminoglycans, proteoglycans, and non-integrin membrane-ECM interactions. In addition, it is also important to highlight the presence of DEGs significantly associated with collagen-containing ECM, cell-cell junctions, and focal adhesion (Fig. 2C). In turn, U251 PrP^C-KO cells presented 363 DEGs, and similar terms were found to be enriched, including those related to metalloendopeptidases, glycosaminoglycans, and metallopeptidases, along with ECM organization and collagen biosynthesis (Fig. 2C).

We filtered DEGs according to their cellular localization and biological processes (BP) using Gene Ontology AmiGO gene sets for a closer examination of the altered genes. As a result, we observed a higher number of DEGs associated with the plasma membrane, cytosol, nucleus, and extracellular milieu in both GBM cell lines (Fig. 2D, E). Moreover, processes such as migration, differentiation, cell adhesion, proliferation, cell-to-cell communication, cell membrane biogenesis and organization, and stemness were altered in PrP^C-KO cells. Interestingly, when analyzing the number

of individual genes, upregulated and downregulated, for each process, U87 PrP^C-KO cells exhibit a high number of upregulated genes related to proliferation, cell-to-cell communication, and membrane organization (Fig. 2D); whereas U251 PrP^C-KO cells display more up-and downregulated DEGs for migration, differentiation and cell adhesion (Fig. 2E).

Figure 2 - Differential gene expression in PrP^{C}-KO GBM cells is associated with cell-to-ECM processes.

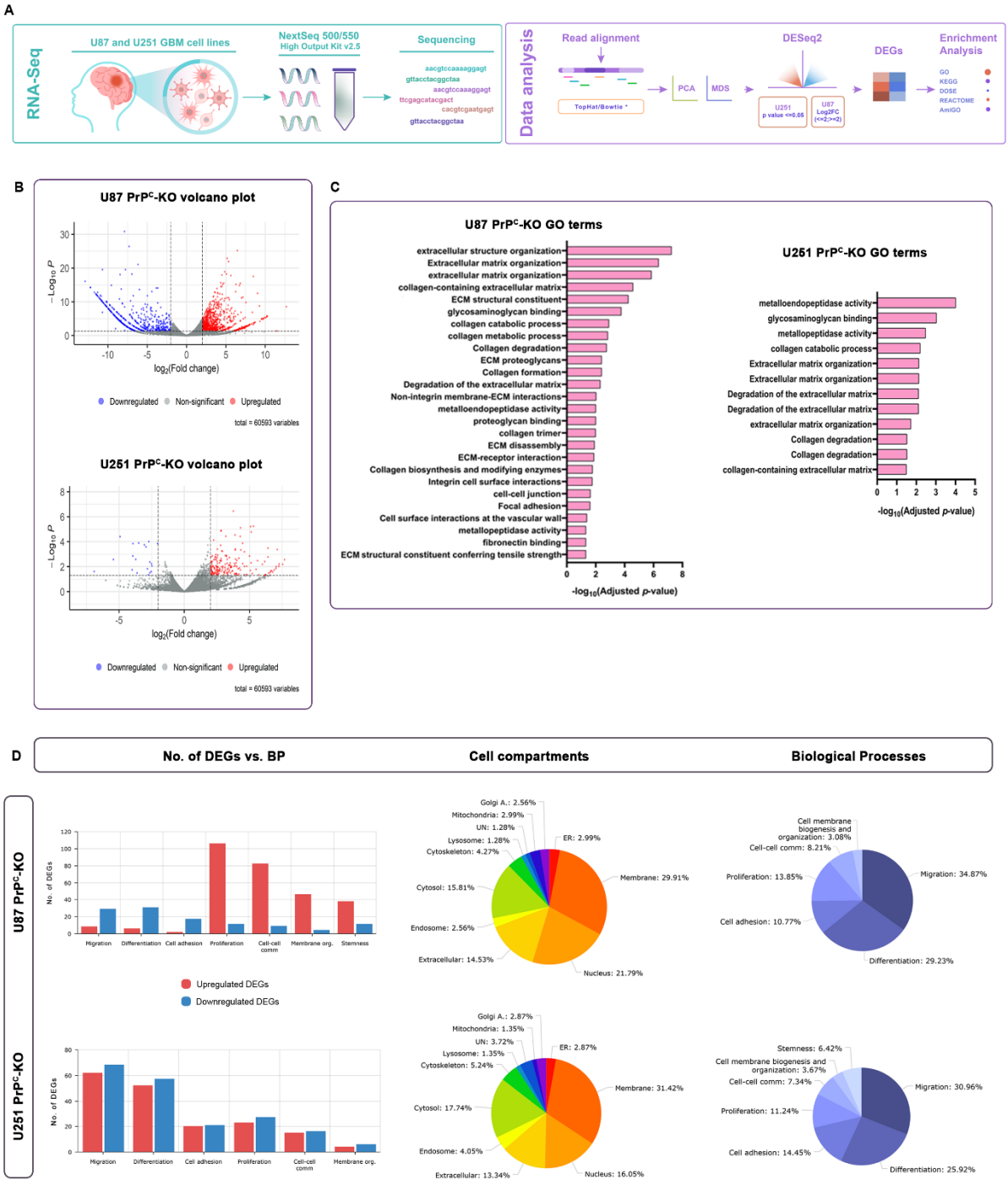

(A) Workflow of the data analysis of RNA-seq for U87 and U251 cells. analysis Workflow. The transcripts with |log2(Fold change)| ≥2 and/or p-value ≤0.05. Read length used was 76 bp, and mean align reads was of 39.23 million, for each sample. (B) Volcano plots of the comparison between wild type U87 and U251 cells versus cellular príon protein knockout (PrPC-KO) cells. The plots depict non-significant (gray), downregulated (blue), and upregulated (red) differentially expressed genes (DEGs). Y-axis shows the mean expression value of log 10 (p-value), and the x-axis displays the log$_2$(foldChange) value. (C) Bar charts show overrepresented terms of Gene Ontology analysis. (D) Biological processes (BP) and cell compartments of U87 and U251 WT vs. PrP^{C}-KO DEGs.

To filter DEGs related to cell adhesion processes, we compared our retrieved DEGs against cell adhesion gene lists from the Gene Ontology AmiGO database. Subsequently, we performed a manual analysis, using information available in the literature, of the filtered gene list by cellular location, general function, specific function in a signaling pathway, association to GBM and to PrP^C. This analysis resulted in several common genes for both groups, highlighting potential targets modulated by *PRNP* expression (Fig. 3A, B). Analysis of these genes' functions suggested that the retrieved gene network participated mainly in axonal growth, cell adhesion, differentiation, and response to environmental cues (Fig. 3C). Given the importance of ITGA6 and PrP^C for the processes highlighted so far and the known relationship between these two molecules, the components of this network represent interesting targets to be closely studied. For instance, the neural cell adhesion molecule NCAM1 is associated with both ITGA6 and PrP^C, as previously described (61)(62). Simultaneously, NCAM1 correlates with the ephrin receptors EPHA4 and EPHB4, which participate in cell morphology, integrin-dependent cell adhesion, and cell-cell signaling (63). Likewise, the relationship of the laminin subunit LAMA5 with ITGA6 and PrP^C is widely described in the literature (65)(66)(67)(17)(68) and can be observed in the network. The observed association points to a network that involves ITGA11, THBS2, and TIMP3, all of them mediators of cell-to-cell and cell-to-matrix interactions (69)(70)(71). The postsynaptic adhesion molecule SLITRK2 and other membrane-associated molecules like APLP1, PARD3B, and MFGE8 were also considered potential targets of interest (Fig. 3B, C). We proceeded with the qPCR validation of DEGs in GBM cell lines to confirm these observations. Paired t-test was performed for statistical analysis of gene expression levels between PrP^C-KO and WT cells. ITGA6 expression appeared downregulated in U87 PrP^C-KO cells (Fig. 3D), while it is upregulated in U251 PrP^C-KO cells (Fig. 3E). LAMA5, THBS2, TIMP3 and NCAM1 were significantly downregulated in both cell lines (Fig. 3D, E). EPHA4 appears downregulated in U87 PrP^C-KO cells (Fig. 3D), and conversely upregulated in U251 PrP^C-KO cells (Fig. 3E).

Even though ITGA6 did not appear as a DEG in our analysis, we were able to validate the relationship of the transcript levels between *ITGA6* and *PRNP* since modulation of ITGA6 expression was observed upon variation of PrP^C expression in

both GBM cell lines. Therefore, these results strengthen the hypothesis of a mechanistically important association between PrP^C and ITGA6 in the GBM context.

Figure 3 - Gene regulatory network directing cell-to-ECM interactions

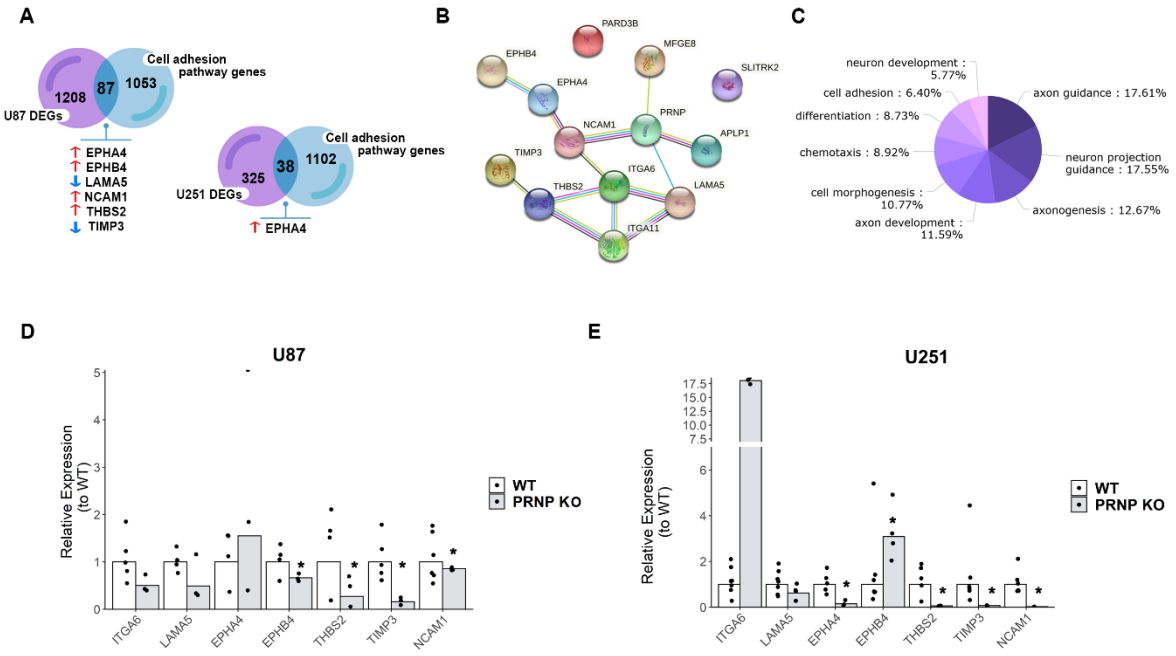

(A) Venn diagram comparing filtered genes for cell adhesion-related pathways and differentially expressed genes (DEGs) from GBM cell lines. Arrows indicate up (red) and down (blue) regulated DEGs. (B) STRING network analysis of cellular prion protein knockout (PrP^C-KO) versus wild-type (WT) DEGs in cell adhesion. Interaction colors are based on published experimental results, with magenta representing experimentally determined interactions, blue represents interactions from curated databases, green represents text mining, black represents co-expression, and purple represents protein homology. (C) Functional enrichment analysis for selected DEGs from A. (D-E) Bar charts of relative expression (qPCR) of selected DEGs for validation in U87 and U251 WT and PrP^C-KO cells. Dots represent individual values. *p<0.05; **p<0.01; ***p<0.001.

4.2 PrP^C and ITGA6 expression in GBM cell lines and patient cells

The leading role of integrins in cell-to-ECM interactions (72), the well-described differential expression of ITGA6 in GBM (24)(42)(73), and its presence within a regulatory network for processes such as adhesion, migration, and differentiation led us to inquire about ITGA6 expression in GBM cell lines, especially in the neurosphere and monolayer condition, since it has been demonstrated that PrP^C is upregulated in neurospheres compared to monolayer culture (10).

Interestingly, ITGA6 expression in U251 cells, known for having a more aggressive phenotype (74), increases in the PrP^C-KO neurospheres (Fig. 4A), whereas ITGA6 expression was not significantly modulated in monolayer cells (Fig. 4B). The protein levels of ITGA6 and PrP^C appeared to be inversely correlated in U251 cells since

ITGA6 expression increased upon knockout of PrP^C, and PrP^C increased upon ITGA6 knockdown (Fig. 4C). Transcript levels of PrP^C in U251cells increase significantly upon ITGA6 overexpression, as well as transcript levels of ITGA6 spike in PrP^C-KO cells (Fig. 4D).

Although ITGA6 total expression levels did not appear to change in the U87 PrP^C-KO monolayer (Fig. 4B), cell surface expression levels of this integrin did increase in U87 neurospheres in the absence of PrP^C (Fig. 4E), aligned with our previous findings. ITGA6 upregulation in neurospheres compared to monolayer cells was corroborated in patient-derived xenografts (PDX) WT cells (Fig. 4F). Interestingly, our group also found that PrP^C is upregulated in the PDX-neurosphere condition (data not shown), suggesting the enrichment of both proteins in stemness maintenance. Indeed, PDX models preserve original tumor characteristics (such as cell heterogeneity, gene signature, tumor architecture, etc.) and represent a gold standard for basic and translational research studies in GBM biology.

Figure 4 - PrP^{C} and integrin α6 expression *in vitro*

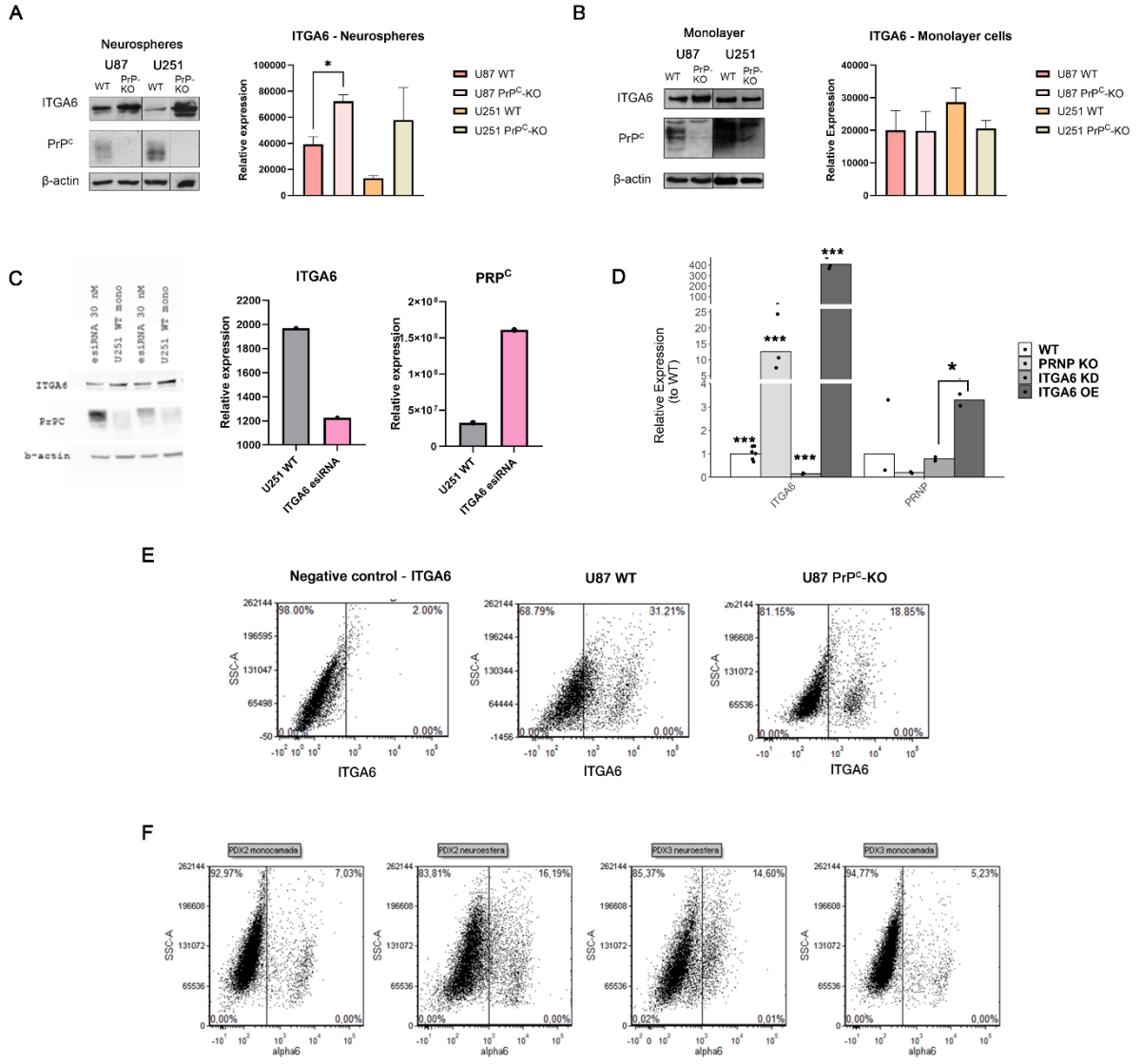

(A) Western blotting analysis of ITGA6 and cellular prion protein (PrP^{C}) in in wild-type (WT) and PrP^{C} knockout (PrP^{C}-KO) U87 and U251 spheres. (B) Western blotting analysis of ITGA6 and PrP^{C} in U87 and U251 WT and PrP^{C}-KO monolayer cells. (C) Effect of ITGA6 knockdown in U87 cells transfected with esiRNA targeting human ITGA6. (D) Bar charts of relative expression (qPCR) of ITGA6 and PrP^{C} in U251 WT, PrPC-KO, ITGA6 knockdown (ITGA6 KD), and ITGA6 overexpressed (ITGA6 OE) cells. Dots represent individual values. *p<0.05; **p<0.01; ***p<0.001. (E) ITGA6 expression in U87 WT (middle) and PrP^{C}-KO- (right) neurospheres. (F) ITGA6 expression in GBM patient xenograft cells (PDX2 or PDX3 cells), showing WT PDX2 monolayer (first panel), WT PDX2 neurospheres (second panel), WT PDX3 monolayer (third panel) and WT PDX3 neurospheres (fourth panel).

Additionally, we assessed protein distribution in GBM neurospheres and monolayer cells labeled with antibodies against ITGA6 and PrP^{C}. We found elevated levels of ITGA6 in conjunction with PrP^{C} expression in U251 WT neurospheres (Fig. 5), suggesting that both molecules are essential for GSCs growth *in vitro*. Remarkably, neurospheres from U251 PrP^{C}-KO cells exhibit an unfitting morphology and even an

absence of cellular protrusions expressing ITGA6, which strengthens the hypothesis of ITGA6 and PrP^C as co-expressing molecules related to dynamic cell membrane structures involved in fundamental processes in GBM, including migration and invasion. Altogether, these results suggest ITGA6 and PrP^C are co-localized in GBM cell lines and specifically upregulated in neurospheres.

Figure 5- ITGA6 and PrP^C co-localization in GBM neurospheres

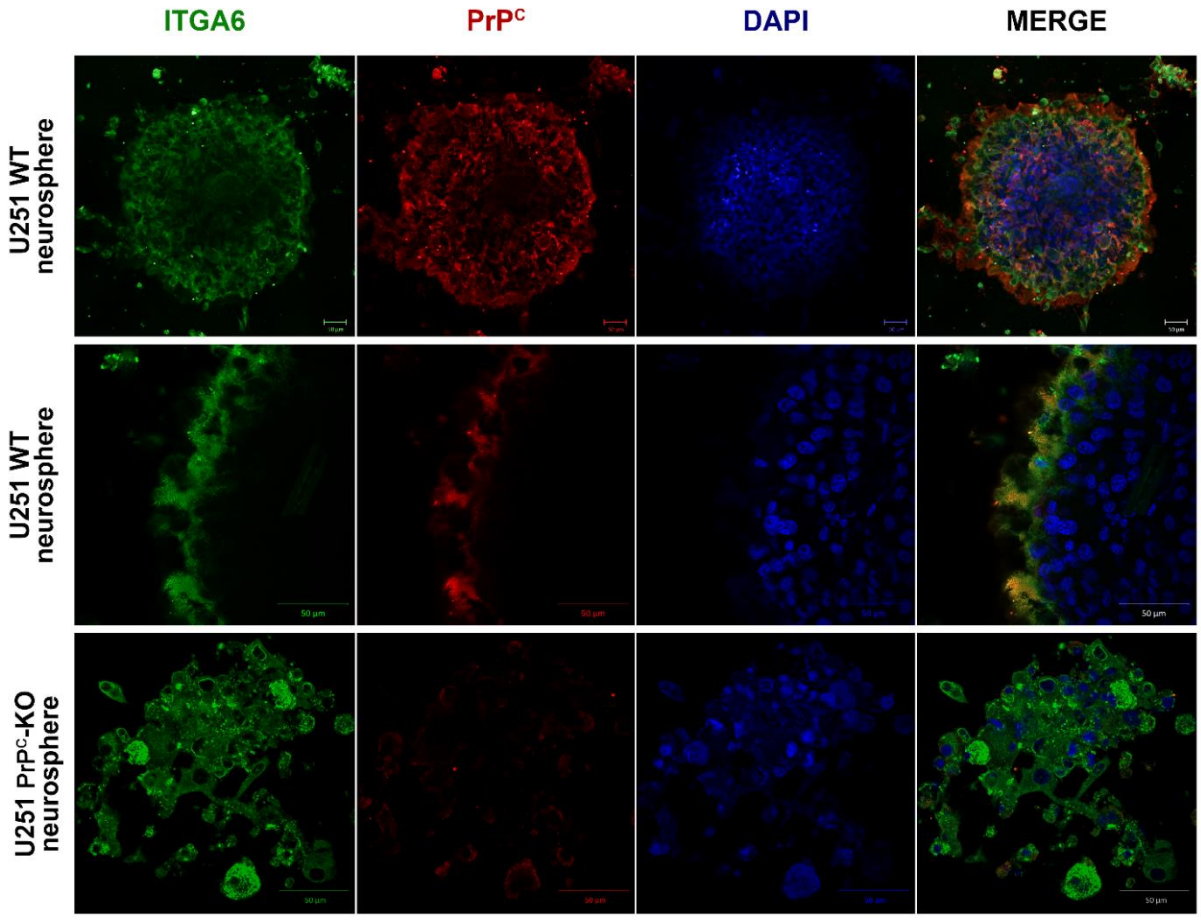

Confocal micrographs of immunostaining analysis from neurospheres: U251 wild-type (WT) (1st and 2nd rows) and cellular prion protein knockout (PrP^C-KO) (3rd row). Nuclei counterstained with DAPI, scale bar = 50 µm.

4.3 Proteome analysis of GBM cells

Seeking to expand the conclusions about the protein levels of these molecules, we performed a meta-analysis using publicly available proteome data and compared the proteome of GBM neurospheres against GBM monolayer cells. ITGA6 appeared as a differentially expressed protein (DEP) (Fig. 6A). Subsequent GO enrichment analysis resulted in several neural ECM-related BP, such as regulation of cell-cell adhesion mediated by integrins, pre-and post-synaptic membrane assembly, neuron development, and other processes related to migration and cell transport (Fig. 6B). Regarding GO cellular components (CC), cell projections, vesicles, and synapses appear among the enriched terms (Fig. 6C).

Figure 6 - Proteomic analysis of GBM neurospheres

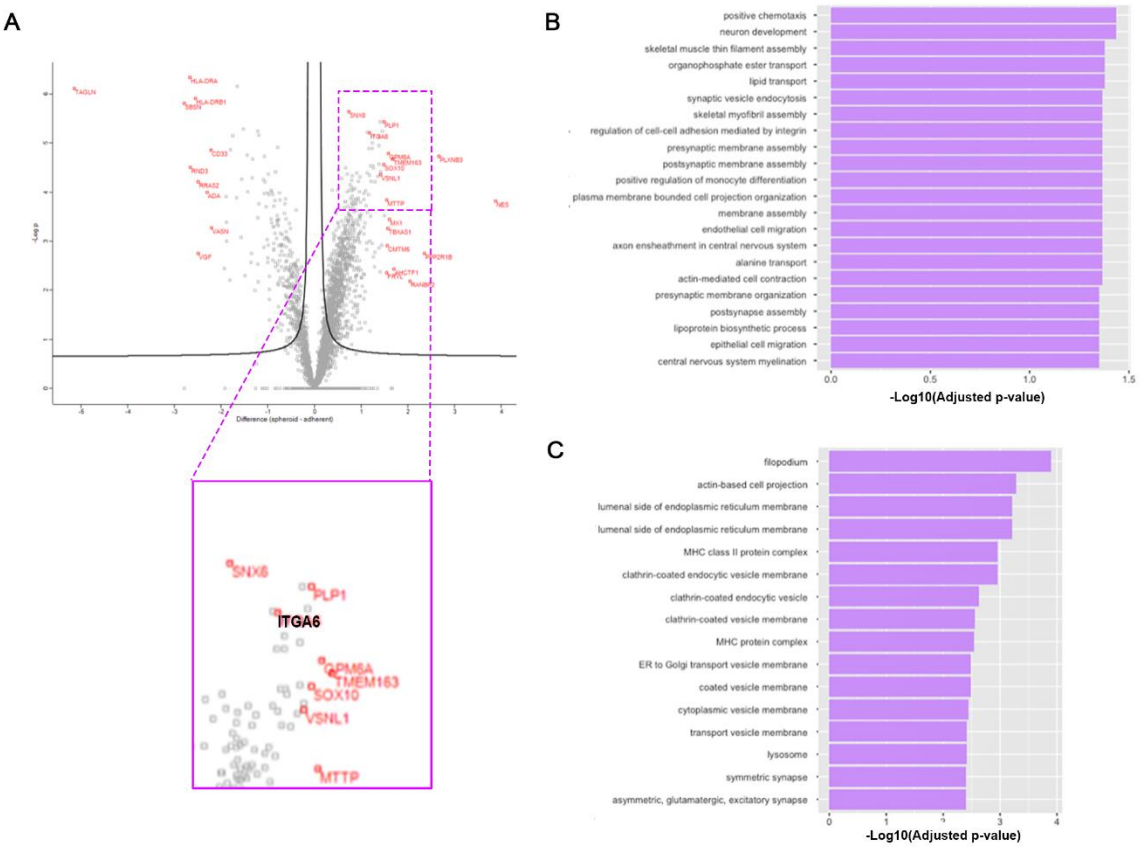

(A)Volcano plot of differentially expressed proteins (DEPs) in in comparison between pool of nurospheres versus monolayer glioblastoma (GBM) cell lines. (B) Bar charts show GO BP from proteomic analysis of GBM neurospheres compared to monolayer cells. (C) Bar charts show GO CC from proteomic analysis of GBM neurospheres compared to monolayer cells.

Moreover, we carried out an additional meta-analysis using patient samples obtained from the PRIDE database. We segregated the GBM samples according to their PrP^{C} (High/Low) or ITGA6 (High/Low) protein levels and performed differential expression analysis (Fig. 7A).

For the ITGA6 comparison, 14 DEPs were obtained (Fig. 7B). BP enrichment analysis showed cell adhesion and ciliary processes involved, while CC showed several endosomal and vesicle components enriched in ITGA6-High patient protein samples (Fig. 7C, D). Interestingly, in our meta-analysis, the ciliary neurotrophic factor receptor (CNTFR) was a downregulated DEP.

For the PrP^C comparison, 489 DEPs were obtained (Fig. 7E), and molecular function and CC enrichment showed processes related to tubulin and microtubule-binding and neuronal components (Fig. 7F, G). Altogether, it is interesting that both ITGA6-High and PrP^C-High samples exhibit DEPs involved in vesicle trafficking, catalytic activity, synaptic cargo transportation, cell adhesion, and cilia-related interactions.

Figure 7 - Differentially expressed proteins (DEPs) in ITGA6-High and PrP^C-High GBM samples

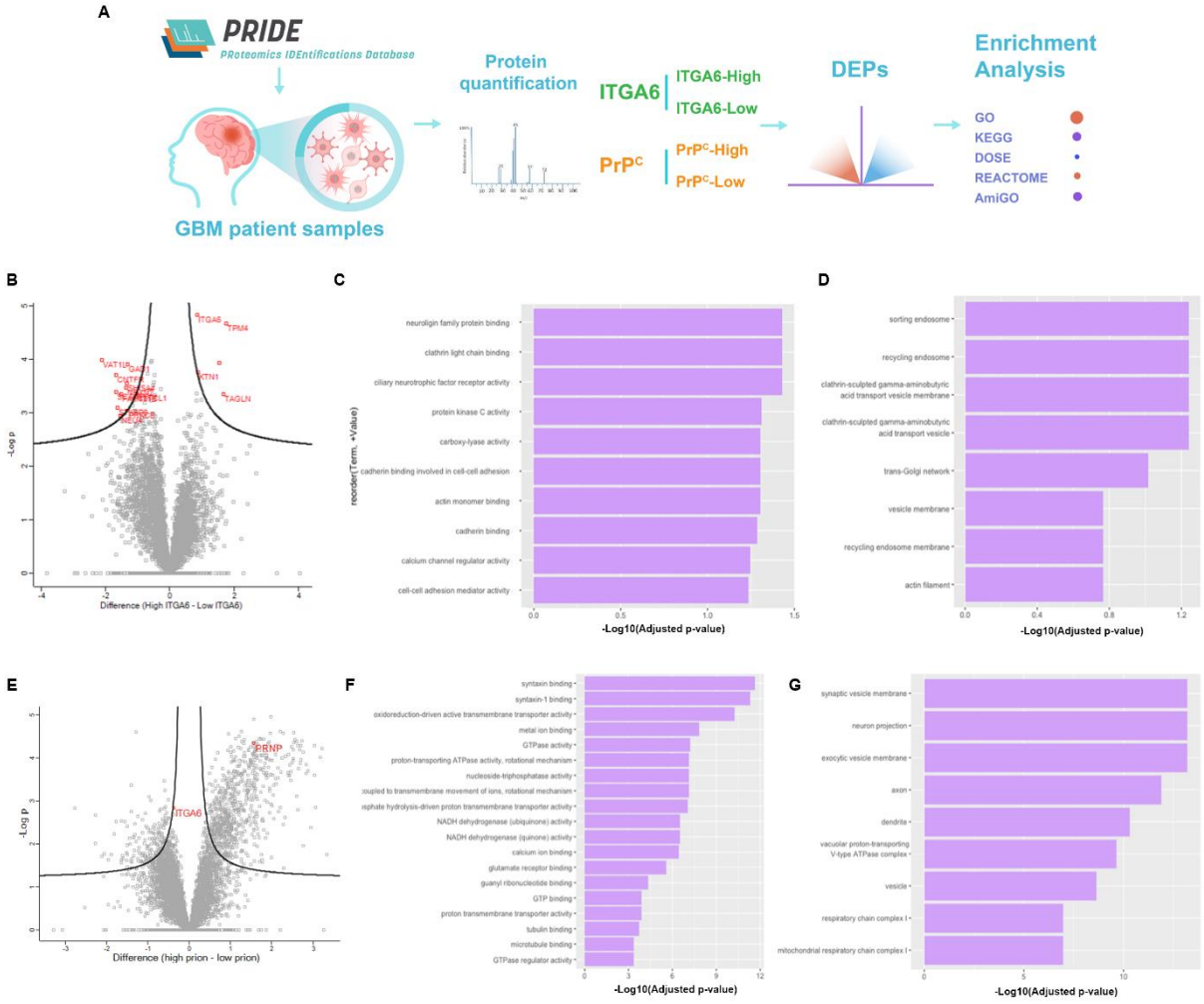

(A) Workflow of the meta-analysis of proteomic glioblastoma (GBM) patient samples. (B) Volcano plot for DEPs in the comparison between ITGA6-High versus ITGA6-Low samples and subsequent (C-D) enrichment analysis. (E) Volcano plot for DEPs the comparison between PrP^C-High versus PrP^C-Low samples and (F-G) subsequent enrichment analysis.

4.4 Transcriptome meta-analysis of ITGA6-High samples

To further validate the clinical relevance of ITGA6 and its potential partners in GBM, we carried out an omics meta-analysis by establishing groups of GBM samples with distinct expressions of *ITGA6*. For the transcriptome meta-analysis, differential gene expression analysis was performed for *ITGA6*-High *vs.* *ITGA6*-Low samples, which were then filtered with both p-adjusted (p-adj) and $\log_2$(foldchange) cutoffs to obtain significant up-and downregulated genes (Fig. 8A). It is noteworthy that the overrepresented DEGs, *DNAAF1, DRC1, DCDC2, RSPH4A, AGR3, ROPN1L, SPAG17, and GAS2L2*, are related to primary cilia and microtubule regulation processes (Fig. 8B, D).

Consistently, CC analysis identified plasma membrane-bounded cell projections as cellular locations of upregulated gene products. Moreover, enrichment analysis in other databases named DO diseases, WikiPathway and Reactome noted conditions like ciliopathies, mental health disorders, brain disease, and NRF2 pathway dysfunction (Fig. 8C, E).

Other strongly upregulated genes such as PCDHGB3 and EGFR are major drivers of cell adhesion, along with cell migration and proliferation mediators like FGFR3 and GRB7 (Fig. 8D). As for the downregulated genes, the majority are associated with cell adhesion, migration, and proliferation, such as LAMB1, COL6A3, DPT, and EREG. The matrix metalloprotease, MMP13, in charge of degrading ECM proteins, was downregulated, together with the cartilage scaffolding gene CILP (Fig. 8D).

BP in ITGA6-High vs. ITGA6-Low downregulated genes were associated with ECM organization, mainly related to collagen, consistent with downregulated genes paired to collagen-rich processes. Furthermore, DEGs related to molecular-level activities performed by ECM structural constituents and metalloproteases were also downregulated. In addition, there were also downregulated genes involved in processes such as stem cell, mesenchymal and neural differentiation (Fig. 8C). As for pathways associated with downregulated genes, we found collagen-related activities and ECM interactions that involve neural adhesion molecules, integrins, metalloproteinases, and GPI-anchored proteins (Fig. 8E). Notably, the enriched BP, pathways, and interactions identified in ITGA6-High vs. ITGA6-Low DEGs are inversely related to enriched

categories in our transcriptomic study of PrP^{C}-KO GBM cells, which once again supports the hypothesis of ITGA6 and PrP^{C} association within a molecular network that participates in critical processes for GBM cells.

Taken together, these results draw attention to primary cilia- and microtubule-based processes as important drivers of cell adhesion, migration, proliferation, and differentiation events in ITGA6-High patient samples, which led us to inquire about the correlation between genes embedded in the categories mentioned above. As a matter of interest, *ITGA6* correlated with *PRNP* and the other 49 genes involved in ciliogenesis (Fig. 8F). Among them are the microtubule-associated protein-coding genes MAP4 and SPEF1, the dynein axonemal heavy chain 7 DNAH7, as well as TTC30A and TTC30B, both participants of cilium formation. Other genes with high correlation code for dynein regulatory complex subunits and dynein assembly factors, such as CCDC113, DNAAF1, and DRC1.

Figure 8- Ciliogenesis and microtubule-related DEGs in ITGA6-High GBM patient samples

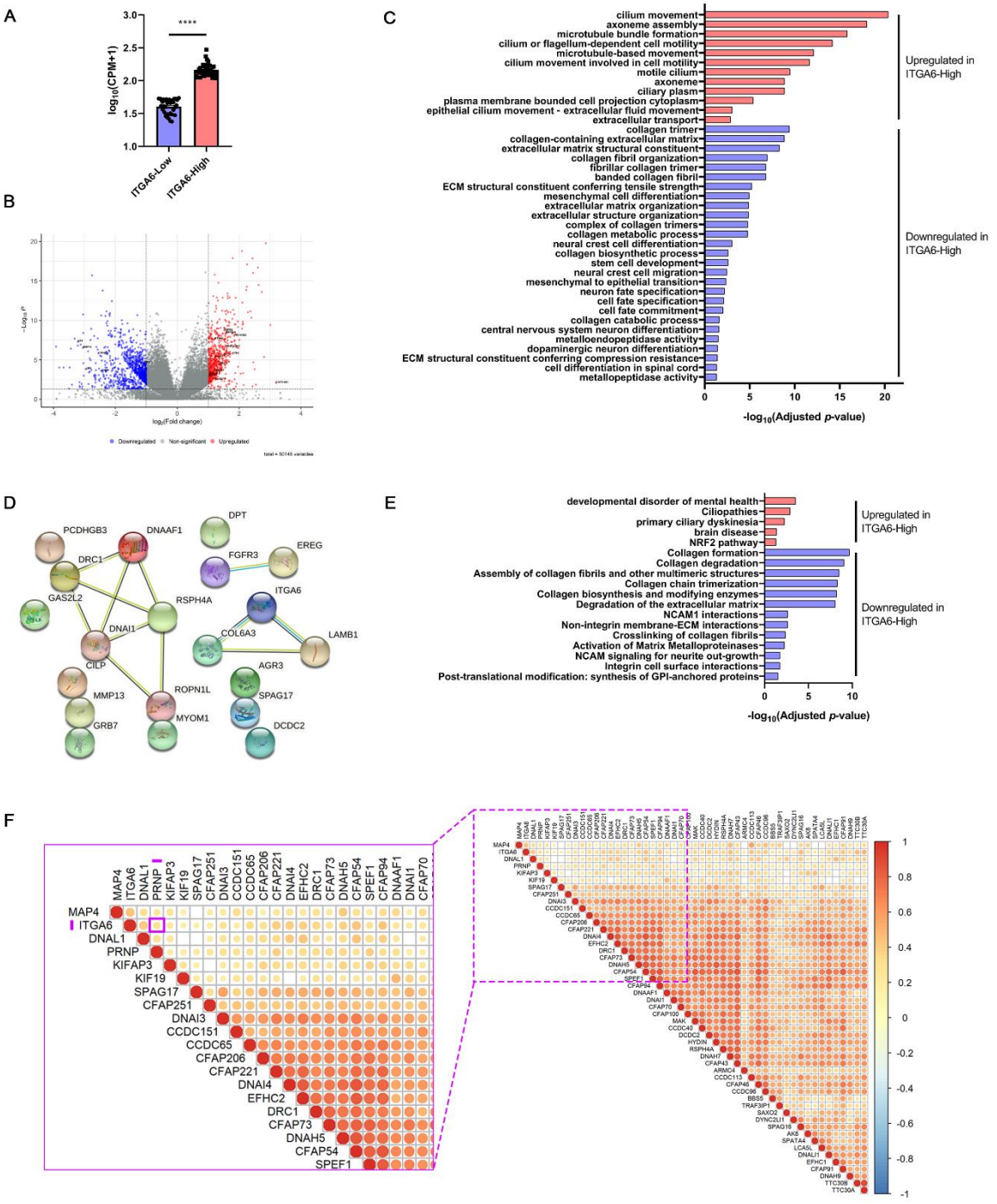

(A) Meta-analysis, barplot displays log10(CPM+1)-normalized ITGA6 counts and demonstrates that the segregation of ITGA6-High and ITGA6-Low patient samples that we performed exhibit differential expression of this gene. According to the Mann-Whitney test, statistical significance was defined as ****p<0.0001. (B) Volcano plots of the comparison between ITGA6-High versus ITGA6-low patient samples. The plots depict non-significant (gray), downregulated (blue), and upregulated (red) differentially expressed genes (DEGs). (C) The bar chart shows GO enrichment analysis in ITGA6-High samples relative to ITGA6-Low. (D) STRING network analysis of ITGA6-High DEGs. (E) The bar chart displays the pathways and diseases related to either up or downregulated ITGA6-High DEGs. (F) The correlation plot demonstrates Spearman correlations ($p<0.05$) between ITGA6, PrP^C, and ciliary plasma-related genes.

4.5 Potential association of ITGA6 and PRNP in primary cilia of GBM cells

Previous works have described the role of primary cilia in directing signaling pathways that influence GBM formation and progression (44). Our transcriptome and proteome analysis of GBM patient samples highlighted several cilia-related DEGs and DEPs within GO categories. Of note, DEGs from primary cilia and microtubule regulation were found in ITGA6-High GBM samples, and 26 DEPs related to ciliary processes were present in PrP^C-High patient samples.

Considering the foregoing results, we filtered the common DEGs between PrP^C-KO GBM cells and cilia-related AmiGO categories to narrow down the list of main gene transcripts that are potential mediators of ciliogenesis within an ITGA6-PRNP hub in GBM cells (Fig. 9A). As a result, 29 DEGs were found for U87 cells and 6 for U251 cells. Among them, the DEGs with the highest fold change shape the main network that highlights several genes established in the literature as known interactors of ITGA6 and PrP^C. Among them, LAMA5; the plasma membrane protrusions gene PROM1, in a sub-network with GLI1, a mediator of SHH signaling and cancer migration; along with the platelet-derived growth factor receptor PDGFRA. Other genes from the main chain are the α-tubulin gene TUBA3C, several genes from the dynein axonemal heavy and light chain, and the axonemal assembly gene TTC29.

We then proceeded with the qPCR validation of the selected cilia-related DEGs in GBM cell lines. Particularly, PDGFRA upregulation in PrP^C-KO U87 cells aligned with the transcriptomic results (Fig. 9B), however, it is noteworthy that PDGFRA expression is the opposite in U251 cells (Fig. 9C). Despite the differences, it is clear that PDGFRA expression seems altered by PrP^C expression. On the other hand, GLI1 expression was significantly downregulated in our qPCR analysis for both cell lines and did not align with the RNA-seq analysis, where it appeared upregulated in PrP^C-KO U87 cells. Regardless, GLI1 expression seems significantly altered by PrP^C expression. As a matter of interest, ITGA6 knockdown (ITGA6 KD) was able to decrease PDGFRA and GLI1 expression (Fig. 9D). ITGA6 overexpression seems to rescue PDGFRA and GLI1 expression compared to PrP^C-KO cells. DNAH1 expression increased upon knockout of PrP^C and significantly dropped upon ITGA6 KD. Finally, TUBA1A expression did not show significant alteration in gene expression (Fig. 9D).

Additionally, we were able to identify primary cilia protruding from the surface of GBM monolayer cells. Primary cilia *in vitro* were counted manually using the cell counter plugin in ImageJ Fiji software. Primary cilia were absent from the neurosphere images, however, the cells in monolayer condition displayed identifiable cilia. We confirmed the expression of α-tubulin labeling the primary cilia in both wild-type and PrP^C-KO cells. Analyses of the number of ciliated cells revealed that 2.48 ± 0.07% of U251 monolayer wild-type cells and 2.45±1.14% of U251 monolayer PrP^C-KO cells were ciliated (mean ± SEM; Fig. 10). These results show that GBM cell lines contain subpopulations of cells that retain their ability to synthesize cilia. Given the limited evidence of primary cilia function associated with the differential expression profile of ITGA6 and PrP^C in GBM cells, further experiments for acetylated α-tubulin detection should be conducted to confirm this.

Figure 9 - Differentially expressed genes (DEGs) related to primary cilia in glioblastoma (GBM) cell lines

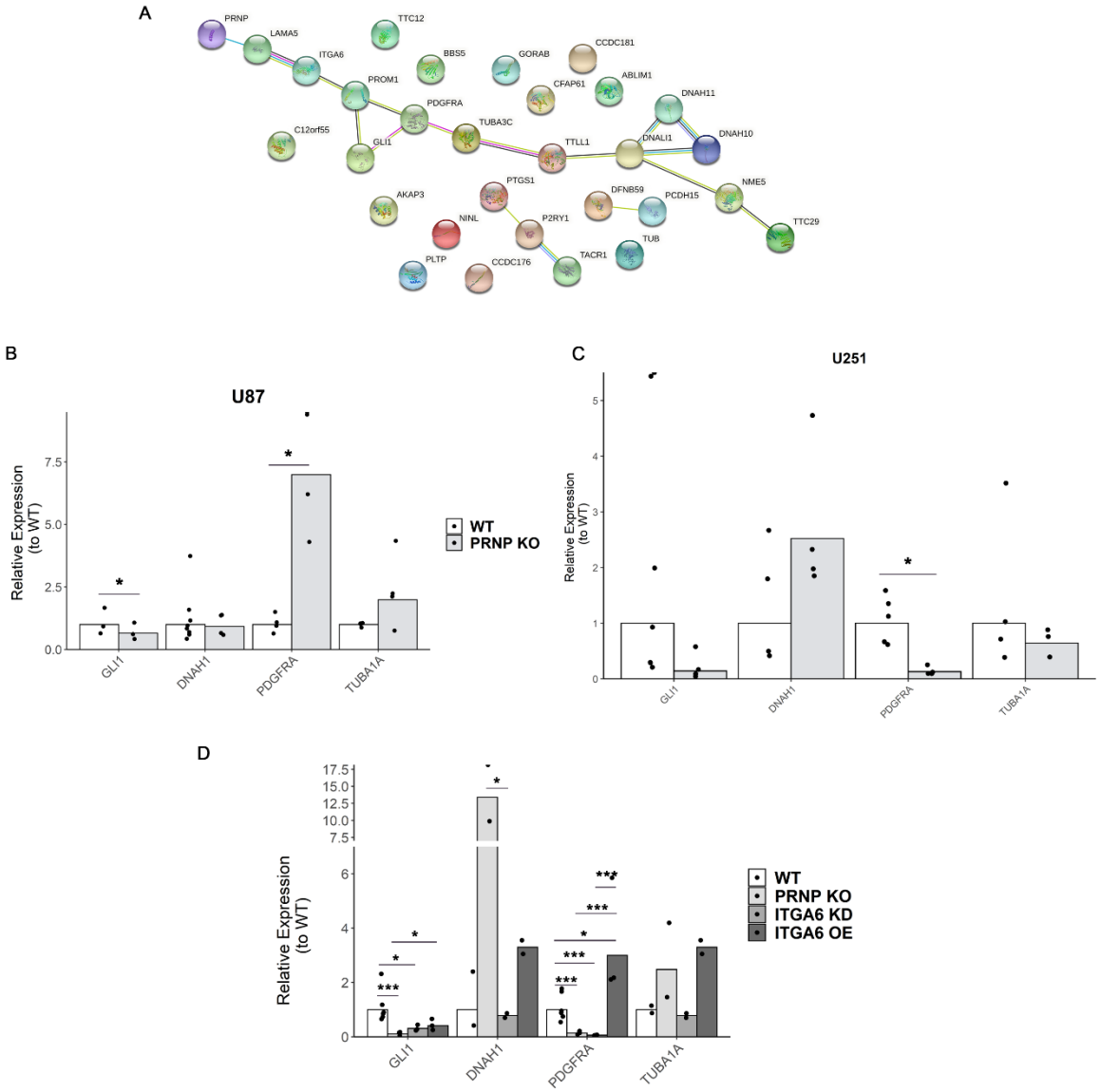

(A) STRING network from DEGs related to primary cilia formation found in transcriptome analysis (Fig. 1). Interaction colors are based on published experimental results, with magenta representing experimentally determined interactions, blue represents interactions from curated databases, green represents text mining, black represents co-expression, and purple represents protein homology. (B-C) Bar charts of relative expression (qPCR) distribution of cilia-related DEGs in U87 and U251 wild-type (WT) and PrP^{C}-KO cells. *p<0.05; **p<0.01; ***p<0.001. (D) Bar charts of relative expression (qPCR) of cilia-related DEGs in U87 and U251 WT, PrP^{C}-KO, ITGA6 knockdown (ITGA6 KD), and cells with overexpression of ITGA6 (ITGA6 OE).

Figure 10 - Detection of primary cilia in glioblastoma (GBM) U251 cell lines

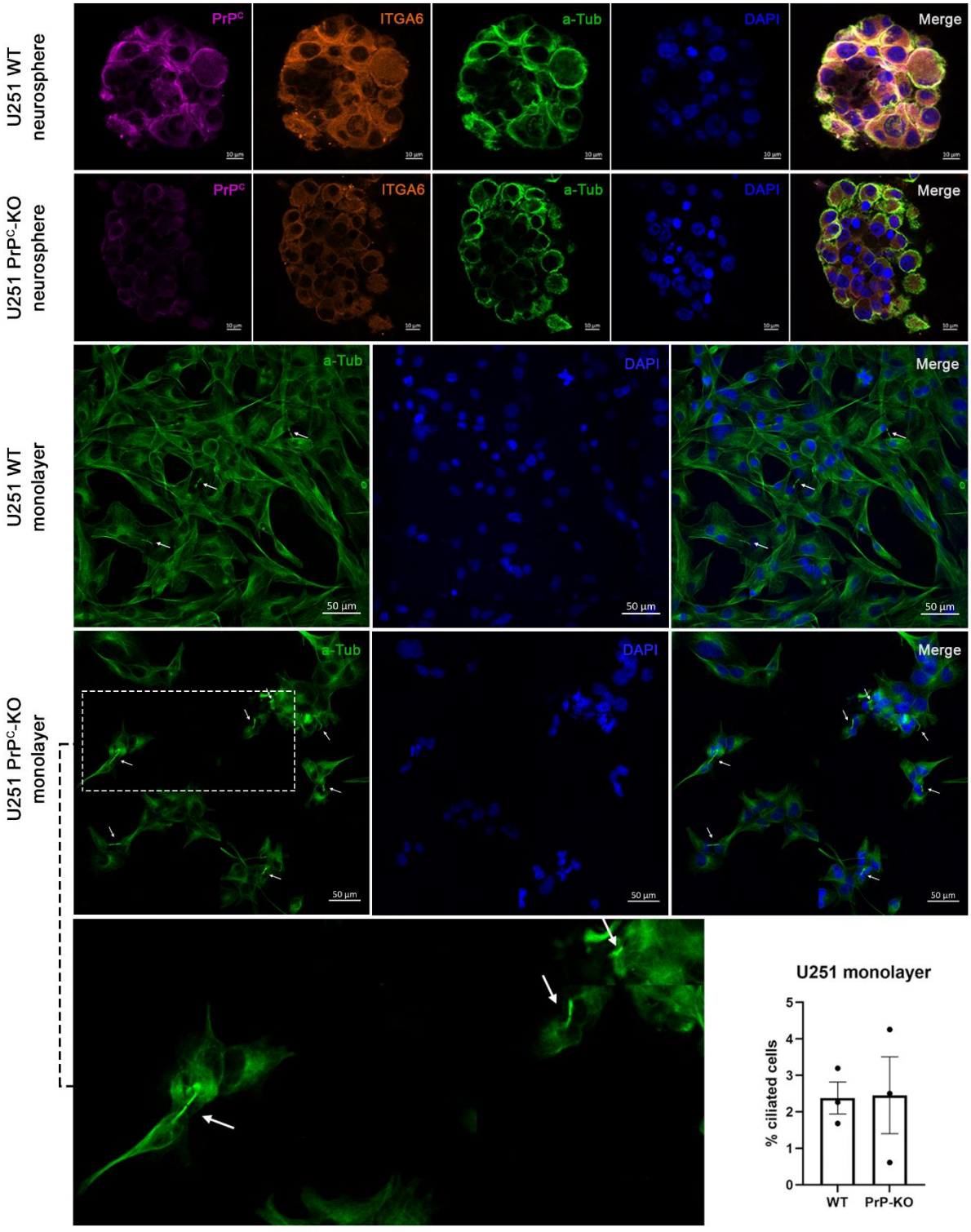

Immunostaining analysis for PrP^C (magenta), integrin α6 (orange), and α-tubulin (green) detection in U251 WT and PrP-KO monolayer and neurosphere cells. Nuclei counterstained with DAPI, scale bar = 50 µm, scale bar for zoom images= 10 µm. Arrows indicate the primary cilia. Bars in lower right corner represent mean percentage (standard error of mean) of α -tubulin + ciliated cells/field for the indicated cells, 24 h after seeding onto glass coverslips.

DISCUSSION

Progress regarding the treatment of GBM is restricted due to the resistance mechanisms of this tumor. The vast intra- and intertumoral heterogeneity of GBM, along with a stem cell-like subpopulation, contribute to therapeutic resistance and prevent complete surgical resection (75). The aggressive nature of GBM is highly determined by several environmental cues that involve both cell-environment and cell-cell contacts (76), which has brought attention to ECM interactions. Integrins are major receptor proteins for cell adhesion that, in turn, modulate signaling cascades that control cell motility, survival, proliferation, and differentiation (77). Specifically, ITGA6 has been described in GBM as a GSCs marker involved in sustaining stemness (24)(42)(73) and even recently described as a mediator of radio-resistance in mesenchymal GSCs (78). Our group has studied the role of PrP^C in GBM as a multivalent scaffold protein binding various extracellular and transmembrane molecules (10)(30)(79). Previous studies have reported PrP^C interacting with laminin (29)(80)(81), NCAM1(82), the amyloid precursor-like protein (APLP1) (83), and the stress-inducible protein 1 (STI1) (84). The present study suggests that ITGA6 may be associated with PrP^C within a regulatory gene network for cell adhesion and cell signaling in GBM cells.

A recent analysis of GBM central tumor samples from both long-term and short-term survivors reported several mRNAs and microRNAs representative of ECM remodeling (85). Several of the highlighted genes encode ECM proteins and/or in the regulation of cell-cell or cell-substrate adhesion, such as collagen IV, CXCL14, and TGFBI. Likewise, ECM remodeling was a key process taking place in our samples. Our results demonstrate that PrP^C-KO GBM cell lines exhibit enrichment of processes tied to ECM and collagen degradation, embedding PrP^C in the cell-to-ECM regulation of GBM cells, specifically in collagen interactions, of which integrins are main recruiters (86).

A further examination into the cell adhesion pathway led us to identify 5 genes that might be at the intersection of the ITGA6-PrP^C context. We validated the differential expression of two ephrin receptors in PrP^C-KO cells. EphA4, for instance, is highly abundant in the brain, prognostic for ovarian and renal cancer, and detected in many cancers, including gliomas (87). EphA4 was found to interfere with integrin signaling pathways, specifically with the subunit of the ITGA6-beta heterodimer, β1-integrin. EphA4 inhibits β1-integrin activity in neuronal cells and induces spine morphological changes, thus modulating synaptic interactions with the extracellular environment (88). Likewise, the other identified ephrin receptor, EphB4, was found to inhibit β1-integrin, and its knockdown induces β8-integrin downregulation (89). It is

important to highlight that PrP^C is a modulator of integrin signaling and other cell surface molecules for processes such as axonal growth (24)(29). β1-integrin aggregation caused by PrP^C depletion has been demonstrated to alter focal adhesions, increase the stability of actin microfilaments, and ultimately impair neurite sprouting (16). In the same manner, the deregulation of the Eph/Ephrin network by PrP^C has been described before, with neurospheres derived from *PRNP*$^{-/-}$ mice embryos and IC11 cells that exhibited strong derangement in a defined set of Eph receptors, including EphB4 (90). In view of the prominent role of these signaling molecules in synaptic plasticity via integrin signaling (91), we speculate that the alterations in Eph signaling may point towards a signaling hub that drives cytoskeleton changes and thus directs processes like migration and cell adhesion.

Another upregulated gene in our samples was THBS2, Thrombospondin 2, that not only regulates cell-cell junctions but also has been proven to inhibit the production of matrix metalloproteinase MMP9 in pancreatic cancer cells. THBS2 is downregulated by miR-744-5p, promoting collagen degradation of basal membranes and thus inducing metastasis (92). THBS2 downregulation in our PrP^C-KO samples is consistent with the overrepresented terms that involve ECM degradation and rearrangement. Concordantly, the tissue inhibitor of metalloprotease TIMP3, an endogenous inhibitor of MMP9 and essential for invadopodia formation in cancer cells (93), appears downregulated in our samples. Similarly, NCAM1, which is highly expressed in GBM and has been associated with infiltrating and immunosuppressive cells (94), appears downregulated in the absence of PrP^C. Altogether the selected cell adhesion DEGs highlight compelling interactions for cell adhesion and cell behavior within the ITGA6-PrP^C network and pathways, as well as a derangement in the cell-cell and cell-ECM processes.

ITGA6 has been well described in GBM due to its high expression and enrichment for GSCs (22). Furthermore, ITGA6 was reported to have a dual role across molecular subtypes by supporting stemness in proneural GSCs while inducing radioresistance in mesenchymal GSCs (78). Thus, we assessed ITGA6 expression *in vitro* in relation to PrP^C expression. Our results indicate that ITGA6 expression is altered at the transcriptional and protein level in PrP^C-KO cells. ITGA6 appears upregulated in U251 PrP^C-KO monolayer cells at the transcriptional level. Likewise, ITGA6 expression increases in U87 PrP^C-KO neurospheres at the protein level and remains upregulated when compared to monolayer cells. Higher expression of ITGA6 and PrP^C in GSCs, when compared to adherent cells, has been reported before (22)(95). Accordingly, our results confirm that WT cells from GBM patient xenografts express more protein levels of

ITGA6 in the neurosphere condition compared to the monolayer condition. Vice versa, upon ITGA6 silencing, PrP^C expression increases in U251 WT monolayer cells. Observed morphological changes in ITGA6 protein distribution of PrP^C-KO neurospheres also contribute to the hypothesis of ITGA6 and PrP^C as collaborative molecules related to dynamic cell membrane structures.

Moreover, our proteome study in the GBM WT pool highlighted the differential expression of ITGA6 in GSC neurospheres versus monolayer cells. The proteome analysis retrieved common terms for both ITGA6-High and PrP^C-High samples, such as membrane-bound endocytic activity, synaptic activities, and membrane transport. The ciliary neurotrophic factor receptor (CNTFR) activity was overrepresented in ITGA6-High samples. CNTFR has been linked to the inhibition of the integrin signaling molecule Focal Adhesion Kinase (FAK) and the downstream c-Jun N-terminal kinase (JNK) for neurogenesis (96). On the other hand, PrP^C-High samples flagged several annotations to synaptic GO terms and synaptic gene sets, which draws attention to the role of both ITGA6 and PrP^C in cell signaling. The present study also extends an earlier proteome analysis that found upregulated expression of ECM-related proteins, such as integrins, laminin subunits, and collagen, in GSCs compared to differentiated GBM cells (97). These GSCs also exhibited higher expression of cell signaling molecules due to the interaction of receptors with the ECM (98), supporting once again a synergic relationship between cell adhesion and cell signaling molecular players in GBM cells.

Particularly, our transcriptome analysis of ITGA6-High samples retrieved downregulated genes in ECM remodeling and collagen-based processes that match the upregulated categories in PrP^C-KO GBM cell lines, making the overrepresentation analyses from ITGA6-High samples and PrP^C-KO GBM cell lines inversely related. Previous works have shown that the molecular composition of ECM contributes to GBM invasiveness (99)(100). Invasion of GBM cells has been linked to upregulated protein expression of matrix metalloproteinases, such as collagenase (MMP1), gelatinase (MMP2 and MMP9), and stromelysin (MMP3) (101). The transcriptomic analysis of ITGA6- and PrP^C-differentially expressed samples flagged several terms associated with dysregulation of the matrix environment and epithelial-mesenchymal transition. Specifically, metalloproteinases and inhibitors of metalloproteinases that have been linked to tumorigenicity and angiogenesis (102), as well as AGR3 are known to participate in the acquisition of a mesenchymal phenotype in cancer, characterized by increased cell motility and resistance to genotoxic agents (103). Two identified DEGs are closely related to ITGA6: the collagen subunit COLA63, which has been

connected to cancer progression by TGF-β-dependent mechanisms, inducing epithelial-mesenchymal transition and fibrosis of the tumor microenvironment (104), and LAMB1 known to be a mesenchymal marker involved in ECM remodeling (105).

Moreover, our correlation analysis from the transcriptome evidenced a relation between ITGA6 and PrP^{C}, along with other DEGs associated with tubulin and microtubule polymerization, specialized coiled coils, such as those found in motor proteins, as well as some DNAH genes that encode the dynein axonemal heavy chain (106). Particularly, DCDC2 is thought to function in neuronal migration, where it may affect primary cilia signaling (107). Previous works approaching the role of cilia in GBM (44) (51) drew our attention to the cilia-related processes that were consistently upregulated in tune with high ITGA6 expression. Differential expression of ITGA6 and PrP^{C} in GBM cells resulted in the identification of candidate players at the center of primary cilium formation, axoneme assembly, cell adhesion, ECM interactions, cell fate commitment, and ciliopathies. These findings fit with previous reports of NEDD9/HEF1-mediated ciliary resorption promoting carcinogenesis by modification of integrin signaling, EMT promotion, secretion of MMPs, and altered ECM (108) (109). Likewise, the ciliary function is altered in PrP-depleted neural tubes that express lower levels of FoxJ1, a transcription factor essential in Shh-mediated ciliogenesis (110). However, studies regarding the ciliary machinery interaction with matrix-regulating processes are limited. Our results highlight the role of a candidate ITGA6-PrP^{C} network in GSCs, which, given their functions in cell-to-ECM interactions, might transduce extracellular signals and integrate them to trigger biological responses in structures of high cell signaling activity such as the primary cilia (Fig. 8).

Integrins and primary cilia have been grouped as mechanosensors (111) and might be involved in monitoring the GBM microenvironment (112). A prior study proved integrin-β1 co-localization with tubulin to the primary cilia involved in fibronectin-induced Ca2+ signaling in Madin-Darby canine kidney cells (113). Likewise, integrin-α3 was located at the primary cilia of smooth muscle cells, and it was shown that collagen-induced [Ca2+] influx response of ciliated cells is blocked under integrin inhibition, suggesting that cilium-located integrins can be activated by ECM components and transduce intracellular signals (111). Further, PrP^{C} depletion has been shown to affect the fine-tuning of tubulin post-translational modifications and cilium-related signaling (58). The pathogenic isoform of the prion protein PrP^{Sc} was associated with the base of cilia (same as the physiological form) and with swollen cone inner segments in retinal structures, suggesting ciliopathy as a pathogenic mechanism (114).

More importantly, one of the main identified DEGs in the proposed ITGA6-PRNP network is PDGFRA, the second most frequently mutated tyrosine kinase receptor, following EGFR, in glioblastomas (115). PDGF-mediated signaling in the primary cilium has been shown to play a critical role in cell growth control (116), and it regulates several functions in the central nervous system such as neurogenesis, cell survival, synaptogenesis, modulation of ligand-gated ion channels, and development of specific types of neurons (117). Additionally, expression of PDGFRA has been reported to be elevated both in malignant as well as in low-grade astrocytoma (114) (118), and a recent study reported that the knockout of PDGFRA in U251 cells inhibits cell growth and invasion *in vitro* and eradicates tumor growth *in vivo* (119). Our results displayed significant changes in PDGFRA expression when ITGA6 and PrP^C expression was modulated, for instance, both the downregulation of ITGA6 and PrP^C decreased PDGFRA expression. Likewise, GLI1, which accumulates at primary cilia to transduce Shh signaling (120), was downregulated in all experimental conditions. Previous studies have described that primary cilia-mediated Shh signaling is required to regulate proliferation and neurogenesis in the ventricular–subventricular zone of the brain (121). Moreover, inhibition of the HH/Gli1 signaling by cyclopamine in U251 cells resulted in increased sensitivity to temozolomide treatment (122).

Among the GLI1 sub-network from our retrieved DEGs, PROM1/CD133, was previously described as a key regulator of ciliary dynamics and sustainment of the normal stem cell quiescence state (123). CD133-KO or overexpression of dominant-negative Prom1 mutant led to the loss of cilium (124). As a matter of interest, PROM1/CD133 is also a conventional GSC marker co-expressed with ITGA6 (22). Other signaling pathways, like Wnt, are tightly related to integrins, and further study would contribute to understanding primary cilia and cell adhesion. Moreover, we reported DEPs from ITGA6-High and PrP^C-High samples involved in vesicle trafficking, calcium channel regulation, cell adhesion, and cilia-related interactions. This is consistent with previous studies describing the co-localization of the recycling endosome marker Rab11 and PrP^C at the ciliary base (58) and Ca2+ signaling response mediated by integrins in the ciliary membrane (38).

Altogether, the alleged localization of ITGA6 and PrP^C at the primary cilia shapes a mechanosensory hub for cell signaling in GBM (Fig. 8) that identify and trigger different pathways and ultimately encompass biological processes like adhesion, survival, migration, and stem-cell maintenance. The present results show that ITGA6 and PrP^C are critical participants of cell adhesion and ciliogenesis in GBM cells by proving their affiliation at the transcriptomic

and proteomic levels in GBM cell lines and across clinical data. The need for adhesion- and signaling-mediated maintenance in cancer cells is well known and motivates future research to inquire about differences in primary cilia among GBM neurospheres and monolayer cells. These findings further suggest that GBM cells' aggressive behavior might be influenced by the primary cilia and partner molecules and thus, point to a new approach for GSCs-targeted therapy.

Figure 11 - Potential role of ITGA6, PrP^{C}, and candidate interactors at the intersection of ciliogenesis and cell adhesion processes in glioblastoma (GBM)

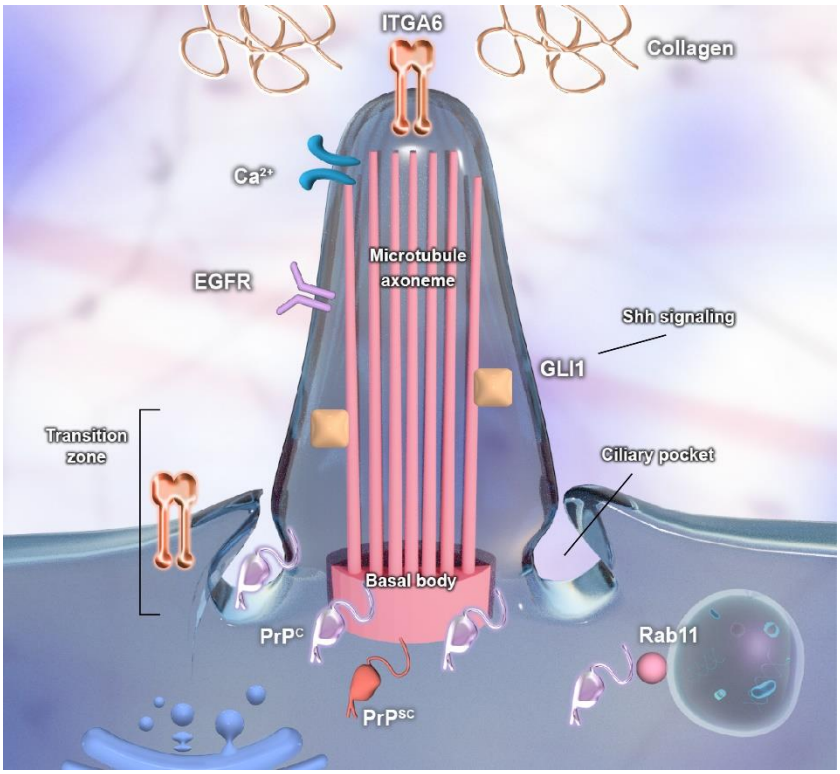

Scheme illustrating how ITGA6 and PrP^{C} might be participants of cell signaling and adhesion processes in the primary cilia of GSCs. ITGA6 might be located at the ciliary membrane or near the transition zone. PrP^{C} is located in the basal body and could be present in the transition zone, specifically in the ciliary pocket. ITGA6 participates in collagen-based processes and may interact with calcium channels and EGFR, the most often mutated protein in GBM. The pathological isoform PrP^{SC} at the basal body might be involved in ciliopathies. ITGA6 and PrP^{C} are linked to vesicle trafficking within the cilia, as well as Shh signaling in GSCs biology. Own work.

5 CONCLUSIONS

I This research aimed to identify a potential interaction between ITGA6 and PrP^C in GBM biology. Based on transcriptomic and proteomic analysis of GBM cell lines, patient samples, and genetic/proteome databases, it can be concluded that ITGA6 and PrP^C are mutually involved in the context of cell adhesion and ciliogenesis in GBM cells.

II The results indicate that:

- PrP^C-KO and ITGA6-High GBM samples flagged terms related to ECM remodeling.
- The retrieved DEGs such as EPHA4, EPHB4, LAMA5, THBS2, and TIMP3 revealed a potential gene network associated with ITGA6 and PrP^C.
- The retrieved DEPs in ITGA6-High samples point to cell adhesion and calcium regulation events, whereas PrP^C-KO samples flagged terms related to cytoskeleton regulation.
- ITGA6 expression is altered at the transcriptional and protein level in PrP^C-KO cells. ITGA6 appears upregulated in PrP^C-KO U251 monolayer cells, and PrP^C is upregulated in ITGA6-knockdown U251 cells at the transcriptional level. Likewise, ITGA6 expression increases in U87 PrP^C-KO neurospheres at the protein level and remains upregulated when compared to monolayer cells.
- Cilia-related genes such as PDGFRA and GLI1 were altered at the transcriptional level upon modulation in the expression of ITGA6 and PrP^C. A cell subpopulation of ciliated cells was identified in WT and PrP^C-KO U251 monolayer cells.

REFERENCES[1]

1. Urbańska K, Sokołowska J, Szmidt M, Sysa P. Glioblastoma multiforme - an overview. Contemp Oncol (Pozn) [Internet]. 2014 [cited 2022 Apr 1];18(5):307–12. Available from: https://pubmed.ncbi.nlm.nih.gov/25477751/

2. Tamimi AF, Department of Neurosurgery, Jordan University Hospital and Medical School, University of Jordan, Amman, Jordan, Juweid M, Department of Radiology and Nuclear Medicine, Jordan University Hospital and Medical School, University of Jordan, Amman, Jordan. Epidemiology and outcome of glioblastoma. In: Glioblastoma. Codon Publications; 2017. p. 143–53.

3. Ferrer VP, Moura Neto V, Mentlein R. Glioma infiltration and extracellular matrix: key players and modulators. Glia [Internet]. 2018;66(8):1542–65. Available from: http://dx.doi.org/10.1002/glia.23309

4. Lee CY. Strategies of temozolomide in future glioblastoma treatment. Onco Targets Ther [Internet]. 2017;10:265–70. Available from: http://dx.doi.org/10.2147/OTT.S120662

5. Yang J, Yang Q. Identification of core genes and screening of potential targets in glioblastoma multiforme by integrated bioinformatic analysis. Front Oncol [Internet]. 2020 [cited 2022 Apr 2];10:615976. Available from: https://pubmed.ncbi.nlm.nih.gov/33718116/

6. Castle AR, Gill AC. Physiological functions of the cellular prion protein. Front Mol Biosci [Internet]. 2017 [cited 2022 Apr 1];4:19. Available from: http://dx.doi.org/10.3389/fmolb.2017.00019

7. Mays CE, Kim C, Haldiman T, van der Merwe J, Lau A, Yang J, et al. Prion disease tempo determined by host-dependent substrate reduction. J Clin Invest [Internet]. 2014 [cited 2022 Apr 1];124(2):847–58. Available from: https://pubmed.ncbi.nlm.nih.gov/24430187/

8. Linden R. The biological function of the prion protein: A cell surface scaffold of signaling modules. Front Mol Neurosci [Internet]. 2017 [cited 2022 Apr 1];10:77. Available from: http://dx.doi.org/10.3389/fnmol.2017.00077

9. Mehrpour M, Codogno P. Prion protein: From physiology to cancer biology. Cancer Lett [Internet]. 2010 [cited 2022 Apr 1];290(1):1–23. Available from: https://pubmed.ncbi.nlm.nih.gov/19674833/

10. Santos TG, Lopes MH, Martins VR. Targeting prion protein interactions in cancer. Prion [Internet]. 2015 [cited 2022 Apr 1];9(3):165–73. Available from: https://pubmed.ncbi.nlm.nih.gov/26110608/

11. Iglesia RP, Prado MB, Cruz L, Martins VR, Santos TG, Lopes MH. Engagement of cellular prion protein with the co-chaperone Hsp70/90 organizing protein regulates the proliferation of glioblastoma stem-like cells. Stem Cell Res Ther [Internet]. 2017 [cited 2022 Apr 1];8(1). Available from: http://dx.doi.org/10.1186/s13287-017-0518-1

[1] Vancouver style

12. Pavon LF, Marti LC, Sibov TT, Malheiros SMF, Brandt RA, Cavalheiro S, et al. In vitro analysis of neurospheres derived from glioblastoma primary culture: A novel methodology paradigm. Front Neurol [Internet]. 2014 [cited 2022 Apr 1];4:214. Available from: https://pubmed.ncbi.nlm.nih.gov/24432012/

13. Baindur-Hudson S, Edkins AL, Blatch GL. Hsp70/Hsp90 organising protein (hop): beyond interactions with chaperones and prion proteins. Subcell Biochem [Internet]. 2015 [cited 2022 Apr 1];78:69–90. Available from: https://pubmed.ncbi.nlm.nih.gov/25487016/

14. Lackie RE, Maciejewski A, Ostapchenko VG, Marques-Lopes J, Choy W-Y, Duennwald ML, et al. The Hsp70/Hsp90 chaperone machinery in neurodegenerative diseases. Front Neurosci [Internet]. 2017;11:254. Available from: http://dx.doi.org/10.3389/fnins.2017.00254

15. Lopes MH, Santos TG, Rodrigues BR, Queiroz-Hazarbassanov N, Cunha IW, Wasilewska-Sampaio AP, et al. Disruption of prion protein-HOP engagement impairs glioblastoma growth and cognitive decline and improves overall survival. Oncogene [Internet]. 2015;34(25):3305–14. Available from: http://dx.doi.org/10.1038/onc.2014.261

16. Loubet D, Dakowski C, Pietri M, Pradines E, Bernard S, Callebert J, et al. Neuritogenesis: the prion protein controls β1 integrin signaling activity. FASEB J [Internet]. 2012 [cited 2022 Apr 1];26(2):678–90. Available from: https://pubmed.ncbi.nlm.nih.gov/22038049/

17. Graner E, Mercadante AF, Zanata SM, Forlenza OV, Cabral AL, Veiga SS, et al. Cellular prion protein binds laminin and mediates neuritogenesis. Brain Res Mol Brain Res [Internet]. 2000 [cited 2022 Apr 1];76(1):85–92. Available from: https://pubmed.ncbi.nlm.nih.gov/10719218/

18. Ma W, Tavakoli T, Derby E, Serebryakova Y, Rao MS, Mattson MP. Cell-extracellular matrix interactions regulate neural differentiation of human embryonic stem cells. BMC Dev Biol [Internet]. 2008;8:90. Available from: http://dx.doi.org/10.1186/1471-213X-8-90

19. Zhou L, Shang Y, Liu C, Li J, Hu H, Liang C, et al. Overexpression of PrPc, combined with MGr1-Ag/37LRP, is predictive of poor prognosis in gastric cancer: PrPc and MGr1-Ag/37LRP predict poor prognosis in GC. Int J Cancer [Internet]. 2014 [cited 2022 Apr 1];135(10):2329–37. Available from: https://pubmed.ncbi.nlm.nih.gov/24706505/

20. Corsini NS, Martin-Villalba A. Integrin alpha 6: anchors away for glioma stem cells. Cell Stem Cell [Internet]. 2010;6(5):403–4. Available from: http://dx.doi.org/10.1016/j.stem.2010.04.003

21. Wilschut KJ, van Tol HTA, Arkesteijn GJA, Haagsman HP, Roelen BAJ. Alpha 6 integrin is important for myogenic stem cell differentiation. Stem Cell Res [Internet]. 2011 [cited 2022 Apr 3];7(2):112–23. Available from: https://pubmed.ncbi.nlm.nih.gov/217636

22. Lathia JD, Gallagher J, Heddleston JM, Wang J, Eyler CE, Macswords J, et al. Integrin alpha 6 regulates glioblastoma stem cells. Cell Stem Cell [Internet]. 2010;6(5):421–32. Available from: http://dx.doi.org/10.1016/j.stem.2010.02.018

23. Kowalski-Chauvel A, Modesto A, Gouaze-Andersson V, Baricault L, Gilhodes J, Delmas C, et al. Alpha-6 integrin promotes radioresistance of glioblastoma by modulating DNA

damage response and the transcription factor Zeb1. Cell Death Dis [Internet]. 2018 [cited 2022 Apr 1];9(9):872. Available from: https://pubmed.ncbi.nlm.nih.gov/30158599/

24. Hajj GNM, Lopes MH, Mercadante AF, Veiga SS, da Silveira RB, Santos TG, et al. Cellular prion protein interaction with vitronectin supports axonal growth and is compensated by integrins. J Cell Sci [Internet]. 2007 [cited 2022 Apr 1];120(Pt 11):1915–26. Available from: https://pubmed.ncbi.nlm.nih.gov/17504807/

25. Peters PJ, Mironov A Jr, Peretz D, van Donselaar E, Leclerc E, Erpel S, et al. Trafficking of prion proteins through a caveolae-mediated endosomal pathway. J Cell Biol [Internet]. 2003 [cited 2022 Apr 3];162(4):703–17. Available from: http://dx.doi.org/10.1083/jcb.200304140

26. Coelho BP, Fernandes CF de L, Boccacino JM, Souza MC da S, Melo-Escobar MI, Alves RN, et al. Multifaceted WNT signaling at the Crossroads between epithelial-mesenchymal transition and autophagy in glioblastoma. Front Oncol [Internet]. 2020;10:597743. Available from: http://dx.doi.org/10.3389/fonc.2020.597743

27. Pai SG, Carneiro BA, Mota JM, Costa R, Leite CA, Barroso-Sousa R, et al. Wnt/beta-catenin pathway: modulating anticancer immune response. J Hematol Oncol [Internet]. 2017;10(1). Available from: http://dx.doi.org/10.1186/s13045-017-0471-6

28. Lee Y, Lee J-K, Ahn SH, Lee J, Nam D-H. WNT signaling in glioblastoma and therapeutic opportunities. Lab Invest [Internet]. 2016;96(2):137–50. Available from: http://dx.doi.org/10.1038/labinvest.2015.140

29. Ghodrati F, Mehrabian M, Williams D, Halgas O, Bourkas MEC, Watts JC, et al. The prion protein is embedded in a molecular environment that modulates transforming growth factor β and integrin signaling. Sci Rep [Internet]. 2018 [cited 2022 Apr 1];8(1). Available from: https://pubmed.ncbi.nlm.nih.gov/29872131/

30. Prado MB, Melo Escobar MI, Alves RN, Coelho BP, Fernandes CF de L, Boccacino JM, et al. Prion protein at the leading edge: Its role in cell motility. Int J Mol Sci [Internet]. 2020 [cited 2022 Apr 1];21(18):6677. Available from: http://dx.doi.org/10.3390/ijms21186677

31. Bodrikov V, Solis GP, Stuermer CAO. Prion protein promotes growth cone development through reggie/flotillin-dependent N-cadherin trafficking. J Neurosci [Internet]. 2011 [cited 2022 Apr 1];31(49):18013–25. Available from: https://pubmed.ncbi.nlm.nih.gov/22159115/

32. Friedl P, Weigelin B. Interstitial leukocyte migration and immune function. Nat Immunol [Internet]. 2008 [cited 2022 Apr 1];9(9):960–9. Available from: https://pubmed.ncbi.nlm.nih.gov/18711433/

33. Richardson DD, Tol S, Valle-Encinas E, Pleguezuelos C, Bierings R, Geerts D, et al. The prion protein inhibits monocytic cell migration by stimulating β1 integrin adhesion and uropod formation. J Cell Sci [Internet]. 2015 [cited 2022 Apr 1];128(16):3018–29. Available from: https://pubmed.ncbi.nlm.nih.gov/26159734/

34. Krebsbach PH, Villa-Diaz LG. The role of integrin α6 (CD49f) in stem cells: More than a conserved biomarker. Stem Cells Dev [Internet]. 2017;26(15):1090–9. Available from: http://dx.doi.org/10.1089/scd.2016.0319

35. Desgrosellier JS, Cheresh DA. Integrins in cancer: biological implications and therapeutic opportunities. Nat Rev Cancer [Internet]. 2010 [cited 2022 Apr 2];10(1):9–22. Available from: https://pubmed.ncbi.nlm.nih.gov/20029421/

36. Sasai N, Briscoe J. Primary cilia and graded Sonic Hedgehog signaling: Primary cilia and graded Sonic Hedgehog signaling. Wiley Interdiscip Rev Dev Biol [Internet]. 2012;1(5):753–72. Available from: http://dx.doi.org/10.1002/wdev.43

37. Seeger-Nukpezah T, Little JL, Serzhanova V, Golemis EA. Cilia and cilia-associated proteins in cancer. Drug Discov Today Dis Mech [Internet]. 2013 [cited 2022 Apr 2];10(3–4):e135–42. Available from: https://pubmed.ncbi.nlm.nih.gov/24982684/

38. Bangs F, Anderson KV. Primary cilia and mammalian Hedgehog signaling. Cold Spring Harb Perspect Biol [Internet]. 2017 [cited 2022 Apr 2];9(5). Available from: https://pubmed.ncbi.nlm.nih.gov/27881449/

39. Yoshimura K, Kawate T, Takeda S. Signaling through the primary cilium affects glial cell survival under a stressed environment. Glia [Internet]. 2011 [cited 2022 Apr 2];59(2):333–44. Available from: https://pubmed.ncbi.nlm.nih.gov/21125655/

40. Sarkisian MR, Siebzehnrubl D, Hoang-Minh L, Deleyrolle L, Silver DJ, Siebzehnrubl FA, et al. Detection of primary cilia in human glioblastoma. J Neurooncol [Internet]. 2014 [cited 2022 Apr 2];117(1):15–24. Available from: https://pubmed.ncbi.nlm.nih.gov/24510433/

41. Yang Y, Roine N, Mäkelä TP. CCRK depletion inhibits glioblastoma cell proliferation in a cilium-dependent manner. EMBO Rep [Internet]. 2013;14(8):741–7. Available from: http://dx.doi.org/10.1038/embor.2013.80

42. Herrmann A, Lahtz C, Song J, Aftabizadeh M, Cherryholmes GA, Xin H, et al. Integrin α6 signaling induces STAT3-TET3-mediated hydroxymethylation of genes critical for maintenance of glioma stem cells. Oncogene [Internet]. 2020;39(10):2156–69. Available from: http://dx.doi.org/10.1038/s41388-019-1134-6

43. Hoang-Minh LB, Deleyrolle LP, Nakamura NS, Parker AK, Martuscello RT, Reynolds BA, et al. PCM1 depletion inhibits glioblastoma cell ciliogenesis and increases cell death and sensitivity to temozolomide. Transl Oncol [Internet]. 2016;9(5):392–402. Available from: http://dx.doi.org/10.1016/j.tranon.2016.08.006

44. Álvarez-Satta M, Matheu A. Primary cilium and glioblastoma. Ther Adv Med Oncol [Internet]. 2018 [cited 2022 Apr 2];10:1758835918801169. Available from: http://dx.doi.org/10.1177/1758835918801169

45. Hua K, Ferland RJ. Primary cilia proteins: ciliary and extraciliary sites and functions. Cell Mol Life Sci [Internet]. 2018;75(9):1521–40. Available from: http://dx.doi.org/10.1007/s00018-017-2740-5

46. Christensen ST, Morthorst SK, Mogensen JB, Pedersen LB. Primary cilia and coordination of receptor tyrosine kinase (RTK) and transforming growth factor β (TGF-β) signaling. Cold Spring Harb Perspect Biol [Internet]. 2017;9(6):a028167. Available from: http://dx.doi.org/10.1101/cshperspect.a028167

47. Grisanti L, Revenkova E, Gordon RE, Iomini C. Primary cilia maintain corneal epithelial homeostasis by regulation of the Notch signaling pathway. Development [Internet]. 2016;143(12):2160–71. Available from: http://dx.doi.org/10.1242/dev.132704

48. Jenks AD, Vyse S, Wong JP, Kostaras E, Keller D, Burgoyne T, et al. Primary cilia mediate diverse kinase inhibitor resistance mechanisms in cancer. Cell Rep [Internet]. 2018;23(10):3042–55. Available from: http://dx.doi.org/10.1016/j.celrep.2018.05.016

49. Youn YH, Han Y-G. Primary cilia in brain development and diseases. Am J Pathol [Internet]. 2018;188(1):11–22. Available from: http://dx.doi.org/10.1016/j.ajpath.2017.08.031

50. Veland IR, Awan A, Pedersen LB, Yoder BK, Christensen ST. Primary cilia and signaling pathways in mammalian development, health and disease. Nephron Physiol [Internet]. 2009;111(3):39–53. Available from: http://dx.doi.org/10.1159/000208212

51. Valente EM, Rosti RO, Gibbs E, Gleeson JG. Primary cilia in neurodevelopmental disorders. Nat Rev Neurol [Internet]. 2014;10(1):27–36. Available from: http://dx.doi.org/10.1038/nrneurol.2013.247

52. Hoang-Minh LB, Deleyrolle LP, Nakamura NS, Parker AK, Martuscello RT, Reynolds BA, et al. PCM1 depletion inhibits glioblastoma cell ciliogenesis and increases cell death and sensitivity to temozolomide. Transl Oncol [Internet]. 2016;9(5):392–402. Available from: http://dx.doi.org/10.1016/j.tranon.2016.08.006

53. Collins I, Wann AKT. Regulation of the extracellular matrix by ciliary machinery. Cells [Internet]. 2020;9(2):278. Available from: http://dx.doi.org/10.3390/cells9020278

54. Seeger-Nukpezah T, Golemis EA. The extracellular matrix and ciliary signaling. Curr Opin Cell Biol [Internet]. 2012;24(5):652–61. Available from: http://dx.doi.org/10.1016/j.ceb.2012.06.002

55. Guemez-Gamboa A, Coufal NG, Gleeson JG. Primary cilia in the developing and mature brain. Neuron [Internet]. 2014 [cited 2022 Apr 4];82(3):511–21. Available from: http://dx.doi.org/10.1016/j.neuron.2014.04.024

56. McGlashan SR, Jensen CG, Poole CA. Localization of extracellular matrix receptors on the chondrocyte primary cilium. J Histochem Cytochem [Internet]. 2006;54(9):1005–14. Available from: http://dx.doi.org/10.1369/jhc.5A6866.2006

57. Kuo J-C. Mechanotransduction at focal adhesions: integrating cytoskeletal mechanics in migrating cells. J Cell Mol Med [Internet]. 2013;17(6):704–12. Available from: http://dx.doi.org/10.1111/jcmm.12054

58. Halliez S, Martin-Lannerée S, Passet B, Hernandez-Rapp J, Castille J, Urien C, et al. Prion protein localizes at the ciliary base during neural and cardiovascular development, and its depletion affects α-tubulin post-translational modifications. Sci Rep [Internet]. 2015;5(1):17146. Available from: http://dx.doi.org/10.1038/srep17146

59. Erhart F, Weiss T, Klingenbrunner S, Fischhuber K, Reitermaier R, Halfmann A, et al. Spheroid glioblastoma culture conditions as antigen source for dendritic cell-based immunotherapy: spheroid proteins are survival-relevant targets but can impair immunogenic

interferon γ production. Cytotherapy [Internet]. 2019;21(6):643–58. Available from: http://dx.doi.org/10.1016/j.jcyt.2019.03.002

60. Oh S, Yeom J, Cho HJ, Kim J-H, Yoon S-J, Kim H, et al. Integrated pharmaco-proteogenomics defines two subgroups in isocitrate dehydrogenase wild-type glioblastoma with prognostic and therapeutic opportunities. Nat Commun [Internet]. 2020;11(1):3288. Available from: http://dx.doi.org/10.1038/s41467-020-17139-y

61. Petridis AK, Nikolopoulos SN, El-Maarouf A. Physical and functional cooperation of neural cell adhesion molecule and β1-integrin in neurite outgrowth induction. J Clin Neurosci [Internet]. 2011;18(8):1109–13. Available from: http://dx.doi.org/10.1016/j.jocn.2010.12.047

62. Santuccione A, Sytnyk V, Leshchyns'ka I, Schachner M. Prion protein recruits its neuronal receptor NCAM to lipid rafts to activate p59fyn and to enhance neurite outgrowth. J Cell Biol [Internet]. 2005;169(2):341–54. Available from: http://dx.doi.org/10.1083/jcb.200409127

63. Royet A, Broutier L, Coissieux M-M, Malleval C, Gadot N, Maillet D, et al. Ephrin-B3 supports glioblastoma growth by inhibiting apoptosis induced by the dependence receptor EphA4. Oncotarget [Internet]. 2017;8(14):23750–9. Available from: http://dx.doi.org/10.18632/oncotarget.16077

64. Friedl P, Mayor R. Tuning collective cell migration by cell–cell junction regulation. Cold Spring Harb Perspect Biol [Internet]. 2017;9(4):a029199. Available from: http://dx.doi.org/10.1101/cshperspect.a029199

65. Li L, Shirkey MW, Zhang T, Xiong Y, Piao W, Saxena V, et al. The lymph node stromal laminin α5 shapes alloimmunity. J Clin Invest [Internet]. 2020;130(5):2602–19. Available from: http://dx.doi.org/10.1172/JCI135099

66. Xu H, Pumiglia K, LaFlamme SE. Laminin-511 and α6 integrins regulate the expression of CXCR4 to promote endothelial morphogenesis. J Cell Sci [Internet]. 2020;133(11):jcs246595. Available from: http://dx.doi.org/10.1242/jcs.246595

67. Rebustini IT, Patel VN, Stewart JS, Layvey A, Georges-Labouesse E, Miner JH, et al. Laminin α5 is necessary for submandibular gland epithelial morphogenesis and influences FGFR expression through β1 integrin signaling. Dev Biol [Internet]. 2007;308(1):15–29. Available from: http://dx.doi.org/10.1016/j.ydbio.2007.04.031

68. Coitinho AS, Freitas ARO, Lopes MH, Hajj GNM, Roesler R, Walz R, et al. The interaction between prion protein and laminin modulates memory consolidation. Eur J Neurosci [Internet]. 2006;24(11):3255–64. Available from: http://dx.doi.org/10.1111/j.1460-9568.2006.05156.x

69. Zhang W-M, Käpylä J, Puranen JS, Knight CG, Tiger C-F, Pentikäinen OT, et al. A11β1 integrin recognizes the GFOGER sequence in interstitial collagens. J Biol Chem [Internet]. 2003;278(9):7270–7. Available from: http://dx.doi.org/10.1074/jbc.m210313200

70. Ao R, Guan L, Wang Y, Wang J-N. Silencing of COL1A2, COL6A3, and THBS2 inhibits gastric cancer cell proliferation, migration, and invasion while promoting apoptosis through the PI3k-Akt signaling pathway. J Cell Biochem [Internet]. 2018;119(6):4420–34. Available from: http://dx.doi.org/10.1002/jcb.26524

71. Jackson HW, Defamie V, Waterhouse P, Khokha R. TIMPs: versatile extracellular regulators in cancer. Nat Rev Cancer [Internet]. 2017;17(1):38–53. Available from: http://dx.doi.org/10.1038/nrc.2016.115

72. Kechagia JZ, Ivaska J, Roca-Cusachs P. Integrins as biomechanical sensors of the microenvironment. Nat Rev Mol Cell Biol [Internet]. 2019;20(8):457–73. Available from: http://dx.doi.org/10.1038/s41580-019-0134-2

73. Velpula KK, Rehman AA, Chelluboina B, Dasari VR, Gondi CS, Rao JS, et al. Glioma stem cell invasion through regulation of the interconnected ERK, integrin α6 and N-cadherin signaling pathway. Cell Signal [Internet]. 2012;24(11):2076–84. Available from: http://dx.doi.org/10.1016/j.cellsig.2012.07.002

74. Qi S, Liu Y. Differences in protein expression between the u251 and u87 cell lines. Turk Neurosurg [Internet]. 2016; Available from: http://dx.doi.org/10.5137/1019-5149.jtn.17746-16.1

75. Bhaduri A, Di Lullo E, Jung D, Müller S, Crouch EE, Espinosa CS, et al. Outer radial Glia-like cancer stem cells contribute to heterogeneity of glioblastoma. Cell Stem Cell [Internet]. 2020;26(1):48-63.e6. Available from: http://dx.doi.org/10.1016/j.stem.2019.11.015

76. Koh I, Cha J, Park J, Choi J, Kang S-G, Kim P. The mode and dynamics of glioblastoma cell invasion into a decellularized tissue-derived extracellular matrix-based three-dimensional tumor model. Sci Rep [Internet]. 2018;8(1). Available from: http://dx.doi.org/10.1038/s41598-018-22681-3

77. Liddington R. Integrins: Molecular and biological responses to the extracellular matrix. Chem Biol [Internet]. 1995;2(8):515–6. Available from: http://dx.doi.org/10.1016/1074-5521(95)90184-1

78. Stanzani E, Pedrosa L, Bourmeau G, Anezo O, Noguera-Castells A, Esteve-Codina A, et al. Dual role of integrin alpha-6 in glioblastoma: Supporting stemness in proneural stem-like cells while inducing radioresistance in mesenchymal stem-like cells. Cancers (Basel) [Internet]. 2021;13(12):3055. Available from: http://dx.doi.org/10.3390/cancers13123055

79. Alves RN, Iglesia RP, Prado MB, Melo Escobar MI, Boccacino JM, Fernandes CF de L, et al. A new take on prion protein dynamics in cellular trafficking. Int J Mol Sci [Internet]. 2020 [cited 2022 Apr 2];21(20):7763. Available from: https://pubmed.ncbi.nlm.nih.gov/33092231/

80. Rieger R, Edenhofer F, Lasmézas CI, Weiss S. The human 37-kDa laminin receptor precursor interacts with the prion protein in eukaryotic cells. Nat Med [Internet]. 1997;3(12):1383–8. Available from: http://dx.doi.org/10.1038/nm1297-1383

81. Dias BDC. Interactions between PrPc and other ligands with the 37-kDa/67-kDa laminin receptor. Front Biosci [Internet]. 2010;15(1):1150. Available from: http://dx.doi.org/10.2741/3667

82. Mehrabian M, Brethour D, Wang H, Xi Z, Rogaeva E, Schmitt-Ulms G. The prion protein controls polysialylation of neural cell adhesion molecule 1 during cellular morphogenesis. PLoS One [Internet]. 2015;10(8):e0133741. Available from: http://dx.doi.org/10.1371/journal.pone.0133741

83. Ruiz-Riquelme A, Lau HHC, Stuart E, Goczi AN, Wang Z, Schmitt-Ulms G, et al. Prion-like propagation of β-amyloid aggregates in the absence of APP overexpression. Acta Neuropathol Commun [Internet]. 2018;6(1). Available from: http://dx.doi.org/10.1186/s40478-018-0529-x

84. Zanata SM, Lopes MH, Mercadante AF, Hajj GNM, Chiarini LB, Nomizo R, et al. Stress-inducible protein 1 is a cell surface ligand for cellular prion that triggers neuroprotection. EMBO J [Internet]. 2002;21(13):3307–16. Available from: http://dx.doi.org/10.1093/emboj/cdf325

85. Fazi B, Felsani A, Grassi L, Moles A, D'Andrea D, Toschi N, et al. The transcriptome and miRNome profiling of glioblastoma tissues and peritumoral regions highlights molecular pathways shared by tumors and surrounding areas and reveals differences between short-term and long-term survivors. Oncotarget [Internet]. 2015 [cited 2022 Apr 3];6(26):22526–52. Available from: https://pubmed.ncbi.nlm.nih.gov/26188123/

86. Jokinen J, Dadu E, Nykvist P, Käpylä J, White DJ, Ivaska J, et al. Integrin-mediated cell adhesion to type I collagen fibrils. J Biol Chem [Internet]. 2004;279(30):31956–63. Available from: http://dx.doi.org/10.1074/jbc.M401409200

87. Zhao J, Stevens CH, Boyd AW, Ooi L, Bartlett PF. Role of EphA4 in mediating motor neuron death in MND. Int J Mol Sci [Internet]. 2021 [cited 2022 Apr 3];22(17):9430. Available from: https://pubmed.ncbi.nlm.nih.gov/34502339/

88. Bourgin C, Murai KK, Richter M, Pasquale EB. The EphA4 receptor regulates dendritic spine remodeling by affecting beta1-integrin signaling pathways. J Cell Biol [Internet]. 2007 [cited 2022 Apr 3];178(7):1295–307. Available from: https://pubmed.ncbi.nlm.nih.gov/17875741/

89. Mertens-Walker I, Fernandini BC, Maharaj MSN, Rockstroh A, Nelson CC, Herington AC, et al. The tumour-promoting receptor tyrosine kinase, EphB4, regulates expression of integrin-β8 in prostate cancer cells. BMC Cancer [Internet]. 2015 [cited 2022 Apr 3];15(1):164. Available from: https://pubmed.ncbi.nlm.nih.gov/25886373/

90. Hirsch TZ, Martin-Lannerée S, Reine F, Hernandez-Rapp J, Herzog L, Dron M, et al. Epigenetic control of the Notch and Eph signaling pathways by the prion protein: Implications for prion diseases. Mol Neurobiol [Internet]. 2019 [cited 2022 Apr 3];56(3):2159–73. Available from: https://pubmed.ncbi.nlm.nih.gov/29998397/

91. Buricchi F, Giannoni E, Grimaldi G, Parri M, Raugei G, Ramponi G, et al. Redox regulation of ephrin/integrin cross-talk. Cell Adh Migr [Internet]. 2007 [cited 2022 Apr 3];1(1):33–42. Available from: https://pubmed.ncbi.nlm.nih.gov/19262085/

92. Jiao H, Zeng L, Zhang J, Yang S, Lou W. THBS2, a microRNA-744-5p target, modulates MMP9 expression through CUX1 in pancreatic neuroendocrine tumors. Oncol Lett [Internet]. 2020 [cited 2022 Apr 3];19(3):1683–92. Available from: https://pubmed.ncbi.nlm.nih.gov/32194660/

93. Bi X, Lou P, Song Y, Sheng X, Liu R, Deng M, et al. Msi1 promotes breast cancer metastasis by regulating invadopodia-mediated extracellular matrix degradation via the Timp3-

Mmp9 pathway. Oncogene [Internet]. 2021 [cited 2022 Apr 3];40(29):4832–45. Available from: https://pubmed.ncbi.nlm.nih.gov/34155343/

94. Schwartzbaum JA, Huang K, Lawler S, Ding B, Yu J, Chiocca EA. Allergy and inflammatory transcriptome is predominantly negatively correlated with CD133 expression in glioblastoma. Neuro Oncol [Internet]. 2010 [cited 2022 Apr 3];12(4):320–7. Available from: https://pubmed.ncbi.nlm.nih.gov/20308310/

95. Corsaro A, Bajetto A, Thellung S, Begani G, Villa V, Nizzari M, et al. Cellular prion protein controls stem cell-like properties of human glioblastoma tumor-initiating cells. Oncotarget [Internet]. 2016;7(25):38638–57. Available from: http://dx.doi.org/10.18632/oncotarget.9575

96. Keasey MP, Kang SS, Lovins C, Hagg T. Inhibition of a novel specific neuroglial integrin signaling pathway increases STAT3-mediated CNTF expression. Cell Commun Signal [Internet]. 2013 [cited 2022 Apr 3];11:35. Available from: https://pubmed.ncbi.nlm.nih.gov/23693126/

97. Fiscon G, Conte F, Licursi V, Nasi S, Paci P. Computational identification of specific genes for glioblastoma stem-like cells identity. Sci Rep [Internet]. 2018;8(1). Available from: http://dx.doi.org/10.1038/s41598-018-26081-5

98. Shevchenko V, Arnotskaya N, Pak O, Sharma A, Sharma HS, Khotimchenko Y, et al. Molecular determinants of the interaction between glioblastoma CD133+ cancer stem cells and the extracellular matrix. Int Rev Neurobiol [Internet]. 2020;151:155–69. Available from: http://dx.doi.org/10.1016/bs.irn.2020.03.005

99. Virga J, Szivos L, Hortobágyi T, Chalsaraei MK, Zahuczky G, Steiner L, et al. Extracellular matrix differences in glioblastoma patients with different prognoses. Oncol Lett [Internet]. 2019 [cited 2022 Apr 3];17(1):797–806. Available from: https://pubmed.ncbi.nlm.nih.gov/30655832/

100. Virga J, Bognár L, Hortobágyi T, Zahuczky G, Csősz É, Kalló G, et al. Prognostic role of the expression of invasion-related molecules in glioblastoma. J Neurol Surg A Cent Eur Neurosurg [Internet]. 2017 [cited 2022 Apr 3];78(1):12–9. Available from: https://pubmed.ncbi.nlm.nih.gov/27529670/

101. Lim E-J, Suh Y, Kim S, Kang S-G, Lee S-J. Force-mediated proinvasive matrix remodeling driven by tumor-associated mesenchymal stem-like cells in glioblastoma. BMB Rep [Internet]. 2018 [cited 2022 Apr 3];51(4):182–7. Available from: https://pubmed.ncbi.nlm.nih.gov/29301607/

102. Pullen NA, Anand M, Cooper PS, Fillmore HL. Matrix metalloproteinase-1 expression enhances tumorigenicity as well as tumor-related angiogenesis and is inversely associated with TIMP-4 expression in a model of glioblastoma. J Neurooncol [Internet]. 2012 [cited 2022 Apr 3];106(3):461–71. Available from: https://pubmed.ncbi.nlm.nih.gov/21858729/

103. Iwadate Y. Epithelial-mesenchymal transition in glioblastoma progression. Oncol Lett [Internet]. 2016 [cited 2022 Apr 3];11(3):1615–20. Available from: https://pubmed.ncbi.nlm.nih.gov/26998052/

104. Wang J, Pan W. The biological role of the collagen alpha-3 (VI) chain and its cleaved C5 domain fragment endotrophin in cancer. Onco Targets Ther [Internet]. 2020 [cited 2022 Apr 3];13:5779–93. Available from: https://pubmed.ncbi.nlm.nih.gov/32606789/

105. Balbous A, Cortes U, Guilloteau K, Villalva C, Flamant S, Gaillard A, et al. A mesenchymal glioma stem cell profile is related to clinical outcome. Oncogenesis [Internet]. 2014 [cited 2022 Apr 3];3(3):e91. Available from: https://pubmed.ncbi.nlm.nih.gov/24637491/

106. Truebestein L, Leonard TA. Coiled-coils: The long and short of it. Bioessays [Internet]. 2016 [cited 2022 Apr 3];38(9):903–16. Available from: https://pubmed.ncbi.nlm.nih.gov/27492088/

107. Massinen S, Hokkanen M-E, Matsson H, Tammimies K, Tapia-Páez I, Dahlström-Heuser V, et al. Increased expression of the dyslexia candidate gene DCDC2 affects length and signaling of primary cilia in neurons. PLoS One [Internet]. 2011 [cited 2022 Apr 3];6(6):e20580. Available from: https://pubmed.ncbi.nlm.nih.gov/21698230/

108. Tikhmyanova N, Golemis EA. NEDD9 and BCAR1 negatively regulate E-cadherin membrane localization, and promote E-cadherin degradation. PLoS One [Internet]. 2011;6(7):e22102. Available from: http://dx.doi.org/10.1371/journal.pone.0022102

109. Pugacheva EN, Jablonski SA, Hartman TR, Henske EP, Golemis EA. HEF1-dependent Aurora A activation induces disassembly of the primary cilium. Cell [Internet]. 2007;129(7):1351–63. Available from: http://dx.doi.org/10.1016/j.cell.2007.04.035

110. Choksi SP, Lauter G, Swoboda P, Roy S. Switching on cilia: transcriptional networks regulating ciliogenesis. Development [Internet]. 2014;141(7):1427–41. Available from: http://dx.doi.org/10.1242/dev.074666

111. Lu CJ, Du H, Wu J, Jansen DA, Jordan KL, Xu N, et al. Non-random distribution and sensory functions of primary cilia in vascular smooth muscle cells. Kidney Blood Press Res [Internet]. 2008;31(3):171–84. Available from: http://dx.doi.org/10.1159/000132462

112. Vaughan TJ, Mullen CA, Verbruggen SW, McNamara LM. Bone cell mechanosensation of fluid flow stimulation: a fluid-structure interaction model characterising the role integrin attachments and primary cilia. Biomech Model Mechanobiol [Internet]. 2015;14(4):703–18. Available from: http://dx.doi.org/10.1007/s10237-014-0631-3

113. Praetorius HA, Praetorius J, Nielsen S, Frokiaer J, Spring KR. Beta1-integrins in the primary cilium of MDCK cells potentiate fibronectin-induced Ca2+ signaling. Am J Physiol Renal Physiol [Internet]. 2004;287(5):F969-78. Available from: http://dx.doi.org/10.1152/ajprenal.00096.2004

114. Striebel JF, Race B, Leung JM, Schwartz C, Chesebro B. Prion-induced photoreceptor degeneration begins with misfolded prion protein accumulation in cones at two distinct sites: cilia and ribbon synapses. Acta Neuropathol Commun [Internet]. 2021;9(1):17. Available from: http://dx.doi.org/10.1186/s40478-021-01120-x

115. Verhaak RGW, Hoadley KA, Purdom E, Wang V, Qi Y, Wilkerson MD, et al. Integrated genomic analysis identifies clinically relevant subtypes of glioblastoma characterized by abnormalities in PDGFRA, IDH1, EGFR, and NF1. Cancer Cell [Internet].

2010 [cited 2022 Apr 3];17(1):98–110. Available from: https://pubmed.ncbi.nlm.nih.gov/20129251/

116. Schneider L, Clement CA, Teilmann SC, Pazour GJ, Hoffmann EK, Satir P, et al. PDGFRalphaalpha signaling is regulated through the primary cilium in fibroblasts. Curr Biol [Internet]. 2005 [cited 2022 Apr 3];15(20):1861–6. Available from: https://pubmed.ncbi.nlm.nih.gov/16243034/

117. Sil S, Periyasamy P, Thangaraj A, Chivero ET, Buch S. PDGF/PDGFR axis in the neural systems. Mol Aspects Med [Internet]. 2018 [cited 2022 Apr 3];62:63–74. Available from: https://pubmed.ncbi.nlm.nih.gov/29409855/

118. Guha A, Dashner K, Black PM, Wagner JA, Stiles CD. Expression of PDGF and PDGF receptors in human astrocytoma operation specimens supports the existence of an autocrine loop. Int J Cancer [Internet]. 1995 [cited 2022 Apr 3];60(2):168–73. Available from: https://pubmed.ncbi.nlm.nih.gov/7829210/

119. Peng G, Wang Y, Ge P, Bailey C, Zhang P, Zhang D, et al. The HIF1α-PDGFD-PDGFRα axis controls glioblastoma growth at normoxia/mild-hypoxia and confers sensitivity to targeted therapy by echinomycin. J Exp Clin Cancer Res [Internet]. 2021 [cited 2022 Apr 3];40(1):278. Available from: https://pubmed.ncbi.nlm.nih.gov/34470658/

120. Han Y, Xiong Y, Shi X, Wu J, Zhao Y, Jiang J. Regulation of Gli ciliary localization and Hedgehog signaling by the PY-NLS/karyopherin-β2 nuclear import system. PLoS Biol [Internet]. 2017;15(8):e2002063. Available from: http://dx.doi.org/10.1371/journal.pbio.2002063

121. Tong CK, Han Y-G, Shah JK, Obernier K, Guinto CD, Alvarez-Buylla A. Primary cilia are required in a unique subpopulation of neural progenitors. Proc Natl Acad Sci U S A [Internet]. 2014;111(34):12438–43. Available from: http://dx.doi.org/10.1073/pnas.1321425111

122. Wang K, Chen D, Qian Z, Cui D, Gao L, Lou M. Hedgehog/Gli1 signaling pathway regulates MGMT expression and chemoresistance to temozolomide in human glioblastoma. Cancer Cell Int [Internet]. 2017 [cited 2022 Apr 3];17:117. Available from: https://pubmed.ncbi.nlm.nih.gov/29225516/

123. Singer D, Thamm K, Zhuang H, Karbanová J, Gao Y, Walker JV, et al. Prominin-1 controls stem cell activation by orchestrating ciliary dynamics. EMBO J [Internet]. 2019;38(2):e99845. Available from: http://dx.doi.org/10.15252/embj.201899845

124. Jászai J, Thamm K, Karbanová J, Janich P, Fargeas CA, Huttner WB, et al. Prominins control ciliary length throughout the animal kingdom: New lessons from human prominin-1 and zebrafish prominin-3. J Biol Chem [Internet]. 2020;295(18):6007–22. Available from: http://dx.doi.org/10.1074/jbc.RA119.011253